ISSN: 1679-3013
D.O.I.: 10.5914/to.2011.0051

SEASONAL AND INTERANNUAL VARIABILITY OF THE SOUTHERN SOUTH EQUATORIAL CURRENT BIFURCATION AND MERIDIONAL TRANSPORT ALONG THE EASTERN BRAZILIAN EDGE.

Doris R. A. **VELEDA**[A]
Moacyr **ARAÚJO**[A]
Marcus **SILVA**[a]
Raul **MONTAGNE**[b]
Rodolfo **ARAÚJO**[a]

Recebido em: 01/12/2010
Aceito em: 06/01/2011

ABSTRACT

The dynamics of the southern band of the South Equatorial Current (sSEC) near to Brazilian shelf is investigated using recent field observations and a regional numerical modeling approach. The field measurements were obtained from five moorings deployed by German CLIVAR (Climate Variability and Predictability Program) cruises (March 2000-August 2004) along a crossshore line at 11oS. The Regional Ocean Model (ROMS) is used to simulate the circulation and thermohaline structures within the ocean area comprised between 5°S-25°S and 20°W-47°W. This integration domain was covered by an isotropic 1/12o horizontal grid and 40 terrain-following layers. The numerical results confirm a seasonal migration of the sSEC divergence along the Brazilian edge, as well as its depth dependence with a maximum southward shift in July at 200 m depth, while a maximum northward displacement occurs in November at this same depth. This intrannual variability coincides with the North Brazil Undercurrent (NBUC) seasonality at 11oS from moorings measurements. Empirical Orthogonal Function (EOF) and numerical results show a minimum NBUC strength during November and a maximum northward transport in July. The mean transport from field measurements is 25Sv while this from numerical simulations is 24.5Sv. The SODA reanalysis with 47 years of monthly mean indicates that the sSEC has not only a seasonal variability as well as quasi-biannual variability.

1. INTRODUCTION

In large parts of the ocean the variability of the flow is much stronger than the mean circulation. Therefore the understanding of the variability of the ocean is crucial for the interpretation of observations and the evaluation of theories. Moreover, the ocean forms the lower boundary of the atmosphere and will directly affect its thermal structure and its water content. This implies that the ocean is not passively driven by the atmosphere, but instead the ocean and the atmosphere should be treated as a coupled system. Furthermore, the knowledge of the South Atlantic circulation variability and itsinteraction with the atmosphere is very limited compared to those of the North Atlantic. It is known that a major portion of variability in the tropical Atlantic currents is considered to be driven by large-scale seasonality in the trade wind regime and the latitude of the Intertropical Convergence Zone (ITCZ) (STRAMMA and SCHOTT, 1999; LUMPKIN and GARZOLI, 2005). Similarly, the dynamics that control the variability in the western boundary regime of the tropical South Atlantic may be a result of the seasonal changes of the surface wind speed. On seasonal time scales the ITCZ migrates northward and southward and leads to changes in the upper ocean parameter distribution and in the

Contato: [a]Laboratório de Oceanografia Física Estuarina e Costeira, Departamento de Oceanografia da Universidade Federal de Pernambuco – LOFEC/DOCEAN/UFPE, Av. Arquitetura s/n, 50740-550, Cidade Universitária, Recife, PE, Brazil

[b]Departamento de Física, Universidade Federal Rural de Pernambuco.

E-Mails: doris.veleda@ufpe.br; moa@ufpe.br; marcus@ufpe.br; montagne@df.ufrpe.br; rodolfo.silva@ufpe.br.

ocean circulation (STRAMMA et al., 2005). The seasonal cycle is the largest atmosphere-ocean signal in the tropical Atlantic (STRAMMA and SCHOTT, 1999). The surface currents reflect the response to the seasonally varying wind field and the migration of the ITCZ. With the ITCZ moving northward from spring to summer, the zonal currents such as the North Equatorial Current (NEC) also move northward.

Besides, the western boundary regime of the tropical South Atlantic Ocean is an important crossroads of inter-hemispheric transfer of warm and cold water masses (BOURLÈS et al., 1999; SCHOTT et al., 2005). The Deep Western Boundary Current (DWBC) transports cold North Atlantic Deep Water (NADW) toward the southern hemisphere, while the North Brazil Undercurrent (NBUC) transports warm surface waters northward to close the thermohaline overturning cell (GORDON, 1986; SCHMITZ, 1995). The pathway that runs into the western boundary regime is a limb of the near surface wind-driven anticyclonic Subtropical gyre (PETERSON and STRAMMA, 1991; STRAMMA and ENGLAND, 1999). The circulation near the surface is dominated by this gyre, which is formed by four different parts. Westward, the southern band of the South Equatorial Current at north, southward the Brazil Current at west, eastward the South Atlantic Current (SAC) at south and northward the Benguela Current at east (STRAMMA and ENGLAND, 1999). The southern limit of this gyre corresponds to the South Atlantic Subtropical Front or Convergence zone. South of the Subtropical Convergence, along the western side of the basin the Falkland Current flows equatorward carrying water from the Antarctic Circumpolar Current. In this area, the Brazil and Falkland Currents converge and the Tropical Surface Water (TSW) and Central high-salinity Waters (SACW) are formed in the South Atlantic. This confluence creates a strong thermohaline front with high temperature gradients, also called the Confluence Front, which is connected to the SAC and recirculates within the southern subtropical gyre and finally, into the southern band of the South Equatorial Current (sSEC) toward the Brazilian shelf (STRAMMA and ENGLAND, 1999). Hence, the sSEC is the major southern pathway by which water is imported into the tropical Atlantic (STRAMMA et al., 2005).

The sSEC is broad and slow flow (STRAMMA et al., 2003; Lumpkin and Garzoli, 2005) transporting subtropical water northwestward into the western Atlantic boundary until it encounters the South American continent. At the easternmost tip of South America the sSEC bifurcates feeding two important western boundary currents. The southward branch is the Brazil Current (BC), initially carrying about 4Sv to the south and northward the sSEC merges with the North Brazil Undercurrent (NBUC), with core velocities of 80 cm s^{-1} near 200 m depth. After passing Cape São Roque at 5°S, the central band of SEC (cSEC) joins the NBUC, causing its vertical structure to change from an undercurrent to a surface-intensified current, namely the North Brazil Current (NBC). The NBC crosses the equator northwestward and retroflects into the zonal equatorial current system (SILVEIRA et al., 1994; STRAMMA et al., 1990, 1995, 2005; SCHOTT et al., 1998). The NBUC has a mean northward transport of ~25.4 Sv along the northern coastline of Brazil and a seasonal cycle of 2.5 Sv amplitude with its northward maximum in July, while the interannual NBUC transport variations are small, varying only by 1.2 Sv, with no detectable trend (SCHOTT et al., 2005). As a western boundary current, the NBUC carries warm waters of the South Atlantic origin across the equator and into the northern hemisphere. It supplies the eastward flow of the South Equatorial Countercurrent (SECC), which partially recirculates into the central band of the SEC (cSEC). Off Brazil, the cSEC forms the surface-intensified NBC west of 35°W, crossing the equator northwestward.

More recently, the sSEC dynamics has received more interest, once it has been evidenced that the sSEC may have an important role on the ocean transport of climatic signals, such as Sea Surface Temperature (SST) anomalies, from the tropical-subtropical region toward the tropics (MALANOTTE-RIZZOLI et al., 2000; STRAMMA et al., 2003). In particular, the region where the sSEC bifurcates is the unites of multiple oceanic-weather forcing of great importance, as (i) transfers of heat and mass between different layers of the tropical Atlantic subsurface; (ii) exchanges of heat and fresh water between the ocean and the atmosphere on the tropical Atlantic surface; (iii) links between climatic

variability of the SST and the heat content of the upper layers of the tropical Atlantic and related atmospheric systems, which controls precipitation on the Brazilian Northeast.

Despite the knowledge of the existence bifurcation and the importance of this phenomenon, the observational and theoretical studies are not yet conclusive. According to Stramma et al. (2003), the large variability of the NBUC at 5°S seems to be linked to equatorial processes, and not to sSEC variability, although the seasonal migration of the sSEC bifurcation (SCHOTT et al., 2005) may be a possible cause of the seasonal cycle of the NBUC at 11ºS.

The bifurcation also affects downstream mesoscale processes in the ocean. For example, in the region south of Cabo Frio (22°S), the BC presents a very energetic pattern, with frequent formation of strong cyclonic and anticyclonic meanders, sometimes detaching from the main flow as well developing rings (CAMPOS et al., 1995). The frequency and intensity of these meso-scale processes are very likely related to the behaviour of the circulation at the sSEC bifurcation. However, the latitude where sSEC bifurcation occurs off Brazil is still poorly known.

Geostrophic flow fields have shown the large-scale behavior of the sSEC in the western South Atlantic, with its axis moving southward at increasing depth. An important result related to this southward shift of the sSEC is its depth dependence of bifurcation latitude along the western boundary. Recently believed, based on the literature, that the sSEC would has a northernmost bifurcation in austral winter and a southernmost bifurcation in austral summer. But the work of Rodrigues et al. (2007) has brought a new perspective to the seasonal variability of sSEC. They have investigated the seasonal variability of the sSEC bifurcation into the BC and NBUC, using a reduced-gravity, primitive equation ocean circulation model to investigate the mean pathways between the South Atlantic subtropical and tropical upper ocean. Their results verify a seasonal strongest variability of the bifurcation latitude in 200 m, where it reaches its southernmost position in July and northernmost position in November. Rodrigues et al. (2007) suggest that a detailed climatology should be constructed from all available historical hydrographic data to investigate the seasonal variability of the sSEC bifurcation from observations.

The western boundary regime of the tropical South Atlantic in its several scales of variability has been the subject of numerous investigations (MOLINARI, 1983; STRAMMA, 1991; STRAMMA et al., 1995; STRAMMA and SCHOTT, 1999; STRAMMA et al., 2005; SCHOTT and BÖNING, 1991; SCHOTT et al., 1993; RHEIN et al., 1995; SCHOTT et al., 2005). The Deep Western Boundary Current (DWBC) transports cold NADW toward the southern hemisphere, while the NBUC flows as a inter-hemispheric conduit of warm surface waters northward to close the thermohaline overturning cell (GORDON, 1986; SCHMITZ, 1995). The SACW, between 100 and 500 m depth, is transported within the sSEC toward the Brazilian shelf, where it is carried toward the equator via NBUC and NBC (STRAMMA and SCHOTT, 1999; STRAMMA et al., 2005).

Furthermore, the flow in the NBUC is of interest for a number of reasons. The upper-layer western boundary flow carried by the NBUC is a crucial link within the Atlantic Subtropical Cell (STC) connecting the subduction regions of the subtropical South Atlantic and the eastward equatorial and off-equatorial undercurrents that supply the equatorial and eastern boundary upwelling regimes. Besides, in the 50–300-m depth range, the NBUC possibly plays an important role in the Atlantic STC.

The STC is one phenomenon that is capable of affecting the tropical SST. It includes all the processes that connect the subtropical ocean to the tropics and thereby determine the water mass structure of the tropical ocean. Moreover, within a STC, subduction processes bring surface waters below the mixed layer, where they will be advected towards the equator. A contribution to comprehend how the boundary regime might be connected to the larger scale circulation of the tropical regime was provided by Schott et al., (2005). They propose that, one possible interpretation for the NBUC seasonal variability is that there is a seasonal migration of the latitude of the sSEC inflow into the

western boundary regime. Another source of seasonal boundary transport variability is the interior Sverdrup transport. Based on the NCEP reanalysis stresses, the Sverdrup transport has a southward maximum in July and a broad minimum during November–May with an annual range of 12 Sv. When they calculated from the scatterometer data, the southward maximum also occurs in July but the annual range was found to be lower, about 8 Sv. The agreement of the southward Sverdrup transport maximum and northward NBUC maximum suggests that the NBUC seasonal cycle may be affected by a response to the interior Sverdrup forcing, but the seasonal curves of NBUC and Sverdrup transport differ. Therefore, they recommend investigating the detailed Rossby wave response in different parts of the basin to wind stress curl forcing at 10°–12°S and how much of observed NBUC variance it may explain.

The goal of this work is to investigate the seasonal and a possible interannual variability of the southern branch of the South Equatorial Current analyzing the structure of the currents at 11°S close to Brazilian coast using a regional oceanic model to confirm the theories about the dynamic of the western boundary regime in the South Atlantic. Additionally, as suggest by literature, the bifurcation of the South Equatorial Current variability is analyzed using climatological data. In the first part of the study a seasonal and intraseasonal variability of the mean flow field at 11°S section is analyzed. The spectral analysis is used to identify the main signals of the currents. Additionally, statistical methods as the Empirical Orthogonal Functions (EOF) are used to evaluate the main patterns of variability in the NBUC at 11°S. The purpose here is to analyze the time variability of the current measurements and to identify the principal modes in which the variations of temperature and current fields are strongly coupled as an indicator of the meridional heat transport. In the second part, the Regional Ocean Modeling System (ROMS) is used for evaluating the seasonal variability of the sSEC divergence off Brazil, and to investigate the circulation structures in the western Atlantic Ocean boundary (5°S -25°S and 20°W-47°W). Model results are compared to field measurements obtained from the current-array moored along a cross-Brazilian-shore transect situated at 11°S. Another contribution of this work is an analysis of the current fields for tropical South Atlantic using results from the Simple Ocean Data Assimilation (SODA) version 2.0.2. A monthly mean of the alongshore current of 47 years is analyzed to identify interannual influences of the sSEC bifurcation.

2. MATERIAL AND METHODS

Study area

The mechanisms of the intraseasonal (ISV), seasonal and interannual variability in the South Atlantic, more precisely the western boundary of the tropical South Atlantic Ocean, along the Brazilian shelf, are studied here. The ocean measurements obtained from five moorings deployed by German CLIVAR (Climate Variability and Predictability Program) are used.

Cross-shore and alongshore components of currents from an array of five current-meter moorings along 225 km across the North Brazil Undercurrent (NBUC) are used describing the structure at 11°S (Figure 2.1).

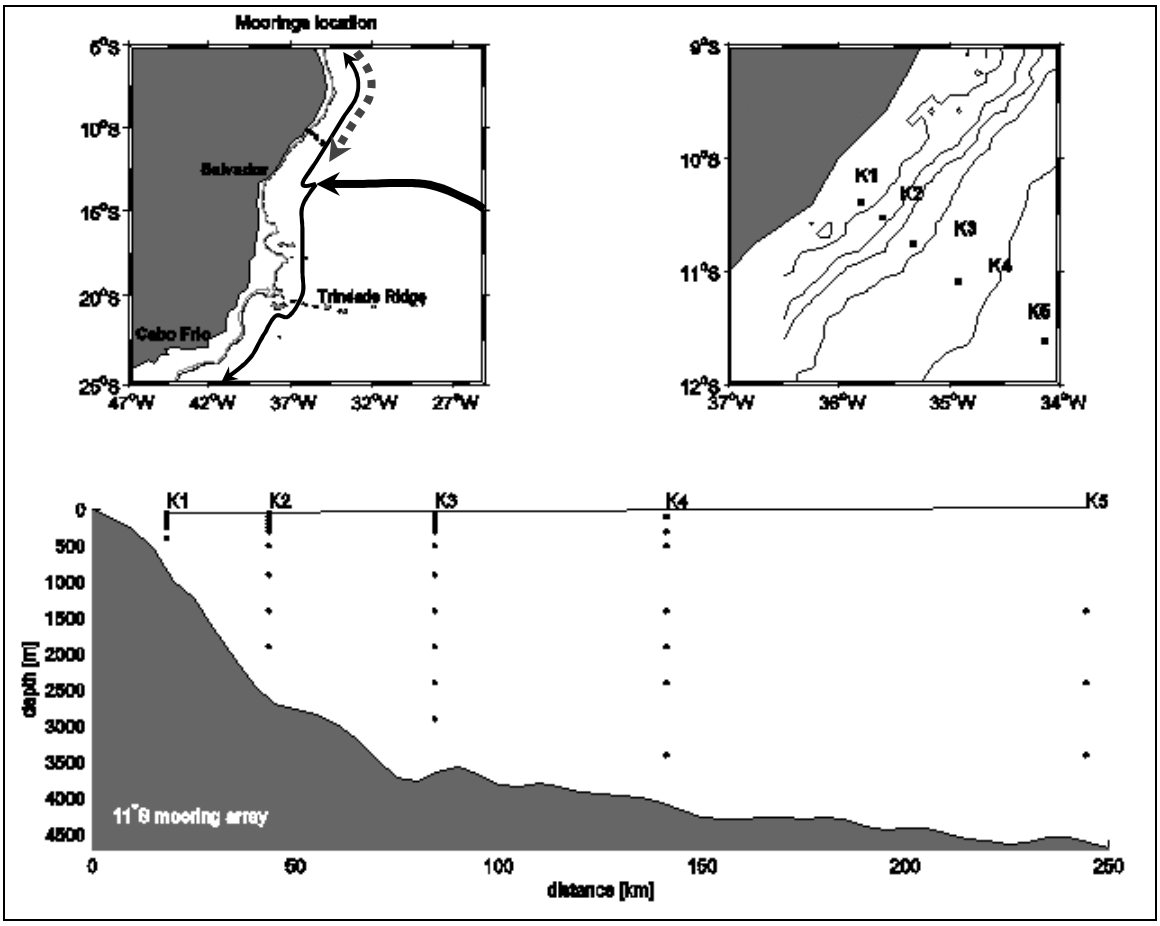

Figure 2.1 – Study area with domain limited by 5° S - 25° S and 20° W - 47° W and location of the K1-K5 moorings along the offshore normal transect about 11°S. Schematic representation of mean meridional transports is indicated: The westward sSEC at 200m depth (large solid line) with the upper ocean northward NBUC flow (solid line), the deepest southward transport by the DWBC (gray dashed line) and southward the BC. At right a panel with a zoom of the moorings position. The lower panel shows the section at 11°S with the distance of the moorings from the coast and instrument depths.

Moored array observations at 11°S

The field data set used here was obtained during the period between March 2000 and August 2004. The data were collected in an array of five current-meter moorings (K1 – K5) along 225 km across the NBUC (10°S - 11°30'S), first deployed in March 2000 by Meteor cruise M47/1. The near-surface flow, at stations K1 – K3, was covered by upward-looking ADCPs, while K4 carried an acoustic current meter at about 100 m depth. Mooring K5 was installed from March 2000 to February 2002 to observe the offshore deep flow. At the deepest levels, currents were recorded by acoustic current meters.

The mooring array was deployed in the western boundary currents crossing the NBUC, which transport the southern waters from South to North Atlantic as a limb of Meridional Overturning Cell (MOC) as a part of the Sub-tropical Cell, that connects the subduction regions of the subtropical South Atlantic and the eastward equatorial and off-equatorial undercurrents that supply the equatorial and eastern boundary upwelling regimes (SCHOTT et al. 2005).

The K1 to K5 mooring lines were used in this work to estimate the monthly-averaged transports at 11°S. These data were also investigated through Principal Component Analysis (PCA) applied for a single field, meridional current only, while K3

and K4 data, for which simultaneous measurements of speed of currents and temperature are available to the same time interval, were also investigated through PCA for coupled fields (Table 1).

Table 1 — Mooring time records, positions, instruments and current-meter depth. For K3 and K4 stations there are temperature measurements for the same time interval and depths.

Station and time period of records	Lat/Lon	Instrument	Depth m
K1 - 02/02/2002 to 17/01/2003 01/06/2003 to 18/08/2004	10° 16.0′ S 35° 51.7′ W	ADCP	32 to 258
K2 - 06/02/2002 to 04/05/2004	10° 22.8′ S 35° 40.8′ W	ADCP	56 to 282
K3 - 21/03/2000 to 31/01/2002 12/05/2003 to 19/08/2004	10° 36.7′ S 35° 23.4′ W	ADCP	29 to 264
		RCM	491 to 2883
		ARGONAUT	888
		FSI-ACM	1386
K4 - 20/03/2000 to 18/08/2004	10° 56.5′ S 34° 59.5′ W	ARGONAUT	112 to 2402
		RCM	
		FSI-ACM	
K5 - 21/03/2000 to 04/02/2002	11° 28.2′ S 34° 12.9′ W	ARGONAUT	1404 to 3404
		FSI-ACM	

These data were also investigated through Spectral Analysis. The data are interpolated to 00 and 12 h. Tidal frequencies are removed from the observed currents by taking a 40 hour filter.

Principal Components Analysis

Principal Components Analysis (PCA) (PREISENDORFER, 1988; JOLLIFFE, 2002) is a method for analysis based on a decomposition of a signal or data set in terms of Proper Orthogonal Decomposition (POD) which are determined from the data. It is the same as performing an Empirical Orthogonal Functions (EOF) analysis on the data, except that in the EOF the components of the basis are continuous instead of discrete as in POD. The PCA is a way of identifying patterns in data, and to analyze its variability. Technically speaking, PCA is a linear transformation that transforms the data to a new coordinate system such that the greatest variance by any projection of the data comes to lie on the first coordinate (called the first principal component), the second greatest variance on the second coordinate, and so on.

Principal Components of velocity data along the 11°S transect and velocity and temperature along the same transect were obtained to provide a compact description of the variability. In this work we compute the Principal Component (PC) for the single field of velocity of the currents and also the PC for the coupled fields of velocity current and temperature.

The PCA applied to the velocity field decomposes the data in an orthogonal basis, with the first mode (the greatest variance mode) corresponding to the first eigenvector of such decomposition and the corresponding eigenvalue giving the variance of this mode.

In general, each the k-th mode e_k accounts for a variance, $\sigma_k = \frac{\lambda_k}{\sum \lambda_i} \times 100$, where λ_k is the eigenvalue of the k[th] eigenvector e_k. In this work, the Singular Value Decomposition algorithm was applied to the sample data to obtain eigenvalues, eigenvectors and time varying amplitudes (PC). The projecting coefficients obtained by the expansion of the sample data onto the eigenvectors, that is the time varying amplitudes, are the principal components, also called expansion coefficients (VAUTARD et al., 1992).

The PCA of the coupled fields of the velocity and the temperature allows the identification of pairs of coupled spatial patterns and their temporal variation, with each pair explaining a fraction of the covariance between the two fields. The methodology is similar to the one described above, the only difference is that, now, the first mode correspond to the greatest variance mode of both fields. In other words, the first mode of the coupled fields corresponds to the mode of the greatest correlation between the two fields. Each pair of data of the two fields corresponds to the same time interval.

The data of the velocity is projected onto the basis generated from the two fields. The same applies for the temperature field. The projecting coefficients obtained by the expansion of the sample data onto the eigenvectors, the principal components (PC), correspond now, to the temporal evolution of the coupling strength between the two fields. The significance of this coupling is characterized by the squared covariance fraction (SCF) explained by each mode. If $\gamma_k = \Gamma(k,k)$ is the i[th] singular value, the fraction of squared covariance (SCF) is given by $SCF_k = \gamma_k^2 / \sum \gamma_k^2$. The coefficient of correlation (CC) of the PC is also calculated to quantify the degree of correlation of the two fields.

The ROMS model

The use of results obtained from numerical simulations has been extremely important for the knowledge of the numerous aspects of the oceanic circulation. The success of the numerical modeling is related to low operational cost and the possibility to study large geographic areas. Based on this premises, this work focus the investigation in a temporal monthly scale, of the velocity and temperature data from the Regional Ocean Modeling System (ROMS).

ROMS has been used to model the circulation in different regions of the world oceans (i.e. HAIDVOGEL et al., 2000; MALANOTTE-RIZZOLI et al., 2000; PENVEN et al., 2000, 2001a,b; MACCREADY and GEYER, 2001; LUTJEHARMS et al., 2003). It solves the free surface with primitive equations in an Earth-centered rotating environment, based on the classical Boussinesq approximation and hydrostatic vertical momentum balance. The model considers coastline and terrain-following curvilinear coordinates, which allows minimizing the number of dead points in computing the solution. The boundary conditions for the model are appropriate for an irregular solid bottom and coastline, free upper surfaces and open-ocean sides away from the coastline. These conditions include the forcing influences of surface wind stress, heat and water fluxes, coastal river inflows, bottom drag, and open-ocean outgoing wave radiation and nudging towards the specified basin-scale circulation. Upstream advection in ROMS is treated with a third-order scheme that enhances the solution through the generation of steep gradients as a function of a given grid size (SHCHEPETKIN and McWILLIAMS, 1998). Unresolved vertical subgrid-scale processes are parameterized by an adaptation of the non-local K-profile planetary boundary layer scheme (LARGE et al., 1994). A complete description of the model may be found in Haidvogel et al. (2000), and Shchepetkin and McWilliams (2003, 2005).

The study presented here deals with the ocean area near the Brazilian coast. Integration domains are comprised within 5°S and 25°S, and 20°W and 47°W (Figure 2.1). An isotropic 1/12° horizontal grid was used for simulations, resulting in 323 x 249 horizontal mesh cells. Vertical discretization considers 40 levels. Bottom topography was derived from a 2' resolution database ETOPO2 (SMITH and SANDWELL, 1997), and a

"slope parameter" $r = \nabla h / h < 0.20$ has been used to prevent errors in the computation of the pressure gradient (HAIDVOGEL et al., 2000). At the three laterals open boundaries (North, East and South) an active, implicit, upstream biased, radiation condition connects the model solution to the ocean surroundings (MARCHESIELLO et al., 2001). Horizontal Laplacian diffusivity inside the integration domain is zero, and a 16-points smooth increasing is imposed (up to 10^4 m^2 s^{-1}) in sponge layers near open ocean boundaries. The model equations were subjected to non-slip boundary conditions at solid boundaries. A basin scale seasonal hydrology derived from WOA 2001 database (monthly climatology at 1° resolution) was used to infer thermodynamics (temperature and salinity) and geostrophy induced currents at the open boundaries. The circulation was forced at the surface by winds, heat fluxes and fresh water fluxes climatology derived from the COADS ocean monthly fluxes data at 0.5° resolution (DA SILVA et al., 1994). The model ran from a state of rest during 10 years. After a spin-up period of about one year, the model has achieved a statistically steady state. All the numerical results examined correspond to the last year of simulation (year 10).

SODA reanalysis data

The Simple Ocean Data Assimilation (SODA) version 2.0.2 is a reanalysis of ocean climate. SODA uses the Geophysical Fluid Dynamics Laboratory-Modular Ocean Model (GFDL-MOM) version 2.2, which is a numerical representation of the ocean's hydrostatic primitive equations. The model is forced by observed surface wind stresses from the COADS data set (from 1958 to 1992) and from NCEP (after 1992). The wind stresses were detrended before use due to inconsistencies with observed sea level pressure trends. The model is also constrained by a sequential data assimilation approach of observed temperatures, salinities, and altimetry using an optimal data assimilation technique, in which a numerical model provides a first guess of the ocean state at the update time. A set of linear Kalman equations is used to correct the first guess. This correction is based on estimates of the errors contained in the model forecast (the difference between the forecast value and true value of a variable such as temperature at a particular location and time) and in the observations. SODA uses advanced error statistics that are flow dependent, anisotropic, and latitude-depth dependent. The observed data comes from: 1) The World Ocean Atlas 1994 which contains ocean temperatures and salinities from mechanical bathythermographs, expendable bathythermographs and conductivity-temperature-depth probes. 2) The expendable bathythermograph archive 3) The TOGA-TAO thermistor array 4) The Soviet Sections tropical program 5) Satellite altimetry from Geosat, ERS/1 and TOPEX/Poseidon. An eddy-permitting reanalysis is based on the Parallel Ocean Program POP-1.4 model with 40 levels in the vertical and a 0.4x0.25 degree displaced pole grid (25 km resolution in the western North Atlantic).

3. RESULTS

The mean boundary current structure at 11°S cross section

In order to describe the mean current regime at 11°S, an average section is calculated from the current measurements. The current vectors are rotated clockwise by an angle of 36° parallel to the coast. The arithmetic mean (2000-2004) of crossshore and alongshore velocity is derived at every instrument depth and onto a regular 5 km by 20 m grid using Gaussian weights (Figure 3.1). Both the crossshore and alongshore mean present maximum velocities centered at about 250 m depth at K2 and K1. At a distance of approximately 20 km from coast, the crossshore component is towards the continent, where the shelf breaks, and positive from here until 100 km reaching to about 1000 m depth. Further down, between K3 and K4, a mean westward crossshore component, towards the continental slope, that associated to the southward alongshore component (Figure 3.1c), confirm the mean southwestward flow, representing the DWBC at 1500-3500 m. The standard deviation shows more crossshore variability from 100 m eastwards K5 (Figure 3.1b). Higher variability is centered at the K4 position at 2000 m depth. In

this position, the eddy model used by Dengler et al. (2004) produced more vigorous eddy activity from April to September.

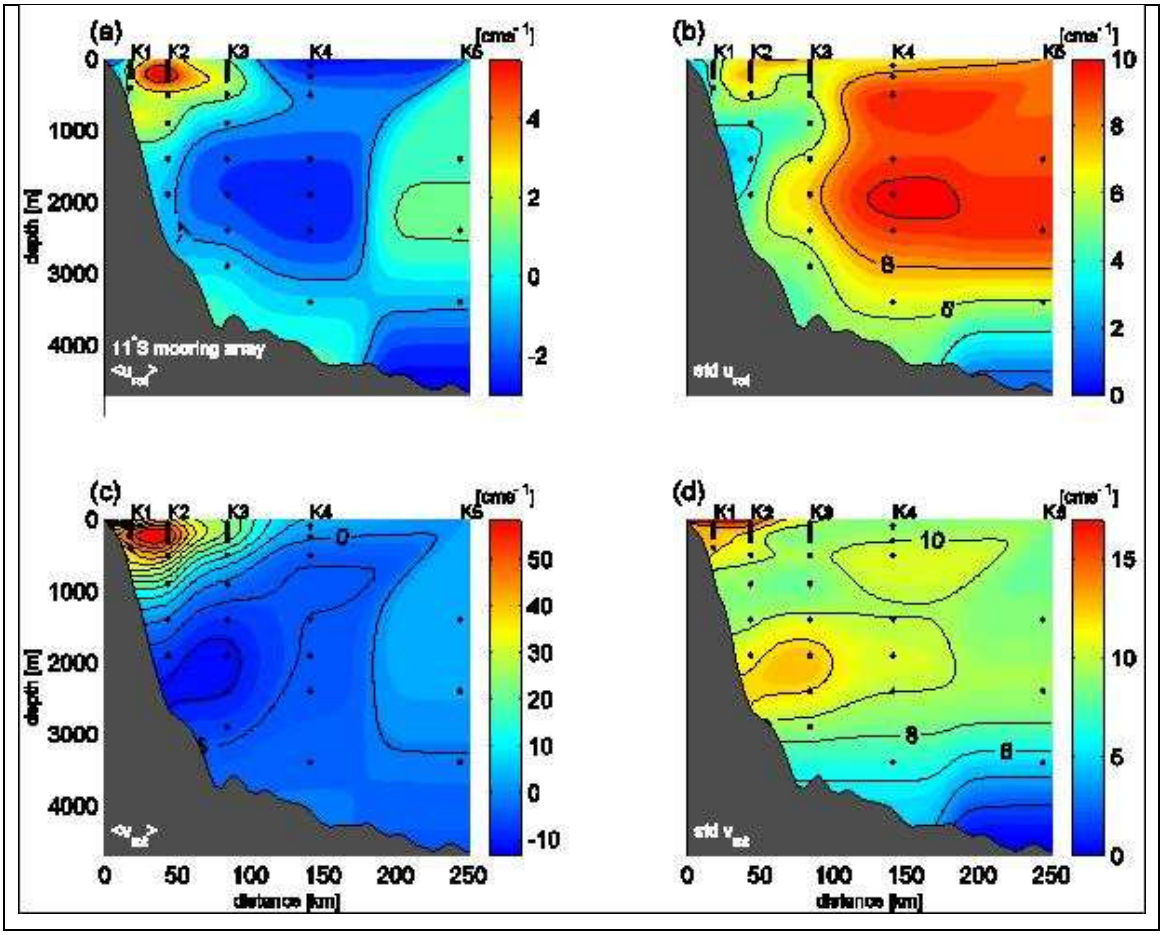

Figure 3.1 – Mean currents: (a) crossshore component, (b) standard deviation of crossshore, (c) alongshore component, (d) standard deviation of alongshore. Instrument depths are marked with a black dot.

In the alongshore component a maximum northeastward core is centered at 250 m depth and situated about 50 km from the coast (Figure 3.1c), where the transport is stronger (SCHOTT et al., 2002; STRAMMA et al., 2003; SCHOTT et al., 2005). This core is associated with the NBUC, which is part of the interhemispheric exchange as the upper limb of the MOC (VON SCHUCKMANN, 2006). The measurements at K3 in the upper 500 m are located at the eastern flank of the NBUC. The mooring K4 is positioned outside the equatorward boundary current. Farther offshore there is a weak mean southward flow (Figure 3.1c) at about 500-1500 m depth which is only covered by mooring K4. The return flow of the MOC, also referred to as the upper limb is compensated with the southward flow of cold water masses in the DWBC. The average current nucleus of the DWBC is centered at mooring K3. The mooring K5 offshore has only provided a two-year-long measurement and the observations are confined to deeper layers below 1500 m while only modest flow exists at K5. There is more variability at the core centered in the NBUC and DWBC, with less but not unnoticed variability is the southward flow at 500-1500 m in K4 position.

Seasonal and intraseasonal variability

The ISV in the near surface layer measurements at 100 m depth will be discussed based on current anomalies are shown in Figure 3.2 at mooring positions K1 to K4 for the years 2000 to 2004. The time series are 40-hour low-pass filtered to eliminate tidal effects and the current vectors are rotated clockwise by an angle of 36° parallel to the

coast. The mean velocities as shown in Figure 3.1 are subtracted, respectively. However, the anomalies at the near shore position K1 show mainly high-frequency variability. Velocity changes sign two to three times a month and the fluctuations exceed 50 cm s^{-1} amplitude. Besides these dominant high-frequency fluctuations, variability exists with periods of 2-3 months (e.g. austral fall to winter 2002). The dominant signal at K2 is characterized by fluctuations with periods of about 2-3 months similar to K1. The amplitudes of the high-frequency (< one month) signal diminish at K2 which consequently means that these fluctuations are confined to the near boundary region. Further offshore two to three monthly fluctuations are again the dominant signal but those amplitudes scale down with increasing distance from the NBUC current core.

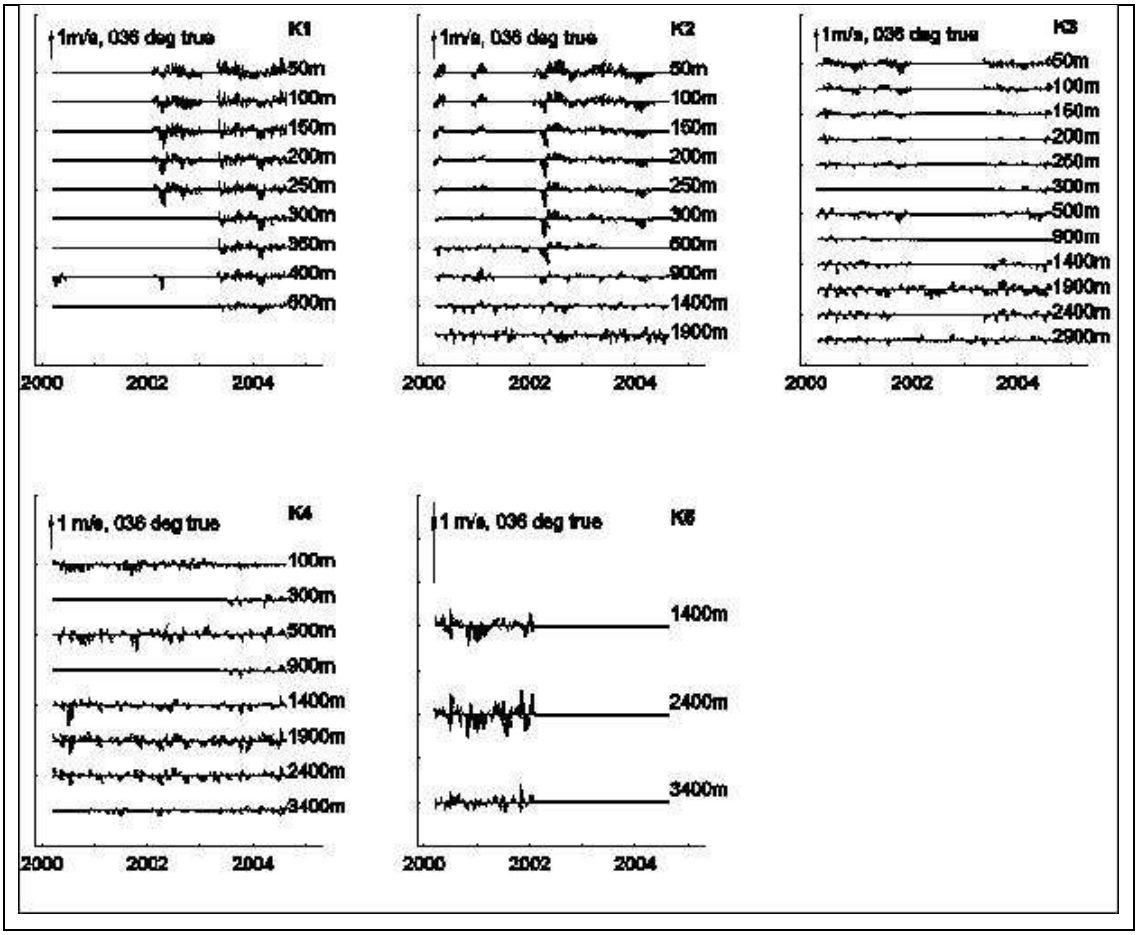

Figure 3.2 – Combined vector time series of 40-hour low-passed current anomalies from March 2000 to August 2004 of the mooring array at 11°S. The time series are rotated 36° parallel to the coast.

For the seasonal alongshore component (Figure 3.3), the strongest values are present in June, July and August, at center of the NBUC. Still, in the upper layers (Figures 3.3e, g) the presence of a mean southward flow at 300-900 m offshore to the NBUC (about 150 km from the coast) is observed. This southward flow offshore to the NBUC was evidenced from field measurements (SCHOTT et al., 2005).

At deeper depths, in the DWBC, the southward center flow is more attached to coast in June, July and August, and broader and weaker in September, October and November. More variability is present for March, April and May, mainly in the NBUC position and DWBC. At K3 position it is pronounced about 2000 m depth in December, January and February. The mean NADW transport is strongest near 2000 m at station K3, and there is mean offshore northward recirculation at 1400 and 2400 m at station K5 (SCHOTT et al., 2005).

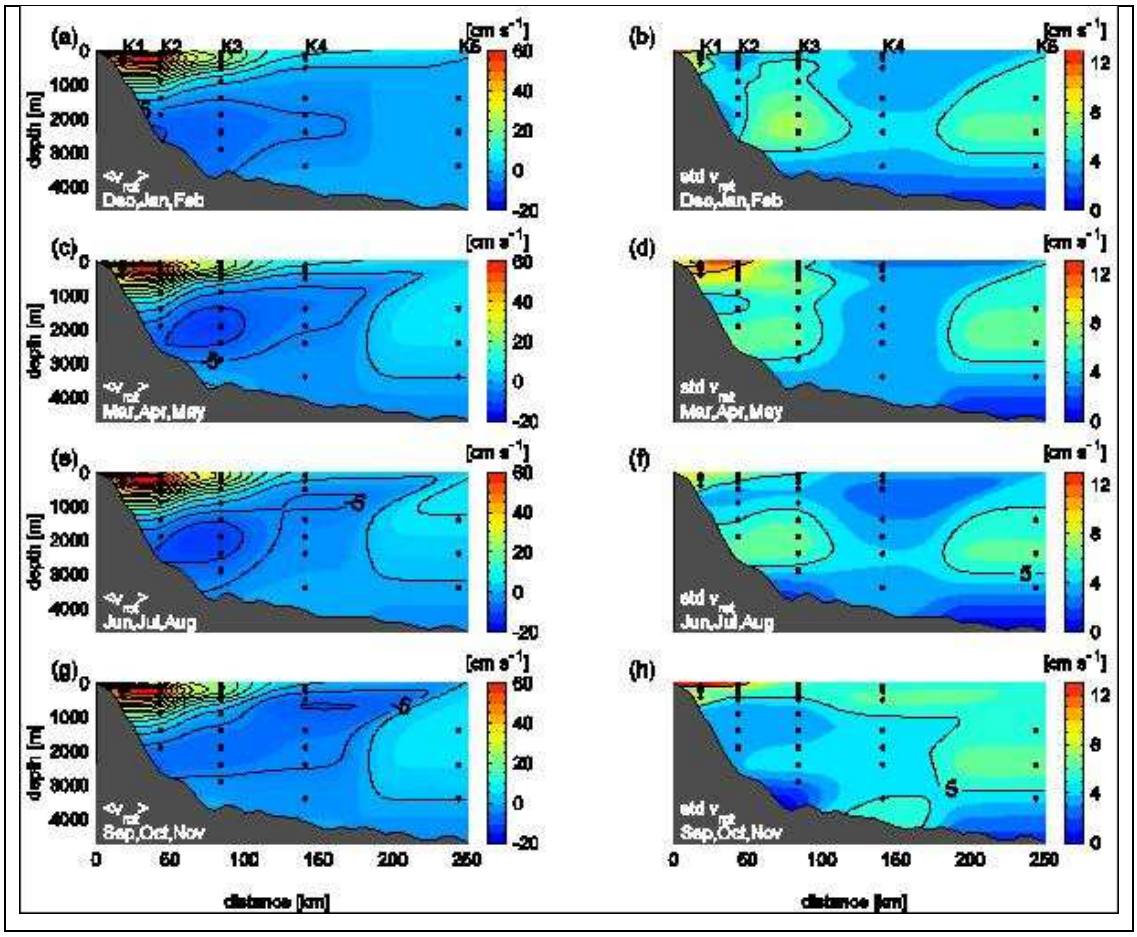

Figure 3.3 – Seasonal alongshore current: (a, c, e, g) mean component, (b, d, f, h) standard deviation.

In the near surface layer, with measurements at 100 m depth from moorings K1-K4 for the years 2000 to 2004, von Schuckmann (2006) has found mainly high-frequency variability in the mooring K1, with velocity changes of 2-3 times a month. Besides these dominant high-frequency fluctuations, there is variability with periods of 2-3 months. The dominant signal at K2 was characterized by fluctuations with periods of about 2-3 months similar to K1. The amplitudes of the high-frequency signal diminish at K2, which means that these fluctuations are confined to the near boundary region. Offshore, the 2-3 months fluctuations are again dominant, but those amplitudes scale with increasing distance from the NBUC core.

The spectral distributions of the current records between 50 and 300 m depth at mooring position K1 to K4 are shown in Figure 3.4. Sections of the time series without interruption are used for spectral analysis. The power spectral density is calculated for each complete part of the combined current meter records with comparable window length and then the average power spectral density is composed in order to determine reliable spectral distributions at each mooring position. For the spectral average the short measurement periods in the years 2000 and 2001 at K2 are neglected for the power spectral density estimates. To preserve the signal variance, under the spectral curve, the power spectral density versus the frequency gives the true signal variance within the band of each frequency interval. Finally, the power spectral density of the cross-shore and alongshore component are summed. In addition, the 95% significance level is dashed for the single spectra at position K1-K4.

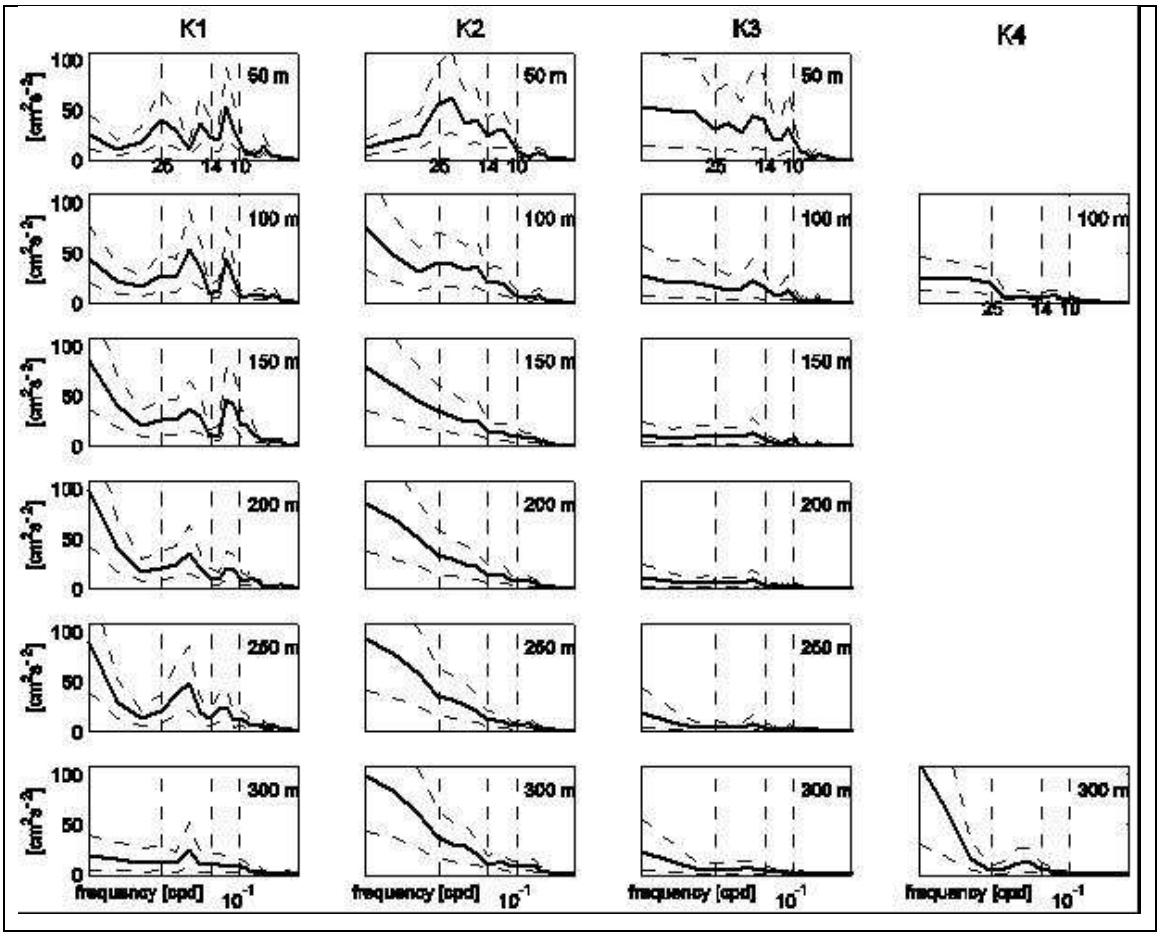

Figure 3.4 – Variance preserving spectrum of kinetic energy [$cm^2\ s^{-2}$] (solid line), for moorings K1-K4, at 50 to 300 m depth, from March 2000 to August 2004, with the respective 95% confidence interval (dashed line).

Significant signals at periods between 10-14 and 14-25 days have been detected in the spectral analysis of current meters at surface as well as at deeper measurements, mainly close to the coast. More variance is dominant at high-frequency in mooring K1, not only at the surface, but it is present at deeper depth, mostly for 10-25 days period. For mooring K2 this high-frequency signal is present at 50 m and 100 m depth, decreasing gradually, with less energy at high-frequencies for deeper depths, where the low-frequency signal is dominant. The high-frequency signal in K2 is about 50% of the variance at lower frequencies. At the mooring K3 this high-frequency signal is present at the surface and gradually decreasing with depth but one peak of energy reaches down to 250 m depth. The variance in K3, for 14-25 days period is dominant at 100-250 m depth. In the mooring K4 the signal at lower frequencies is dominant but at 300 m depth one peak of energy, at 14-25 days is also present. The high-frequency signals are evident mostly close to coast, at mooring K1. Further offshore this signal is more apparent at upper depths and these amplitudes scale down with increasing distance from the NBUC current core.

EOF applied to moorings at 11°S section

The empirical Orthogonal Functions analysis of the meridional component of current fields (from now on called *current)* were computed in K1, K2, K3 and K4 moorings to provide a simpler description of their variability. Usually, most of the variance of the spatially distributed time series is retained in the first few EOFs functions. In this study, a singular value decomposition of the data matrix was used to obtain eigenvalues, eigenvectors and time varying amplitudes, or principal components, of the sample covariance matrix. ' summarizes the results of EOF analysis for the meridional component of current fields from the moorings. A single field analysis was done for those

stations.

Table 2 – EOF analysis applied to the meridional component of the current at 11°S. The SFC is Squared Fraction Covariance for each mode in meridional velocity of current from mooring data. The column "Period (days)" shows the periodicity of the maximum variance for each mode in single field analysis.

Mooring	EOF Mode	SCF (%)	Period (days)	Depth (m)
K1	1°	90	14-25-60	300
	2°	10	60	100
K2	1°	99	14-25-60	50-200
K3	1°	63	14-25	100
	2°	34	14	300-500
K4	1°	81	14-30-60	1900
	2°	14	60	500
K5	1°	97	25-60	2400

The K1 mooring is located at approximately 10 km from the coast, which goes northward in the boundary western regime. The first EOF mode is allocated at approximately 300 m depth and account for 90% of the total variance. The spectrum clearly shows dominant mode of variability at 14-25 days. The second mode for K1, with only 10% of the total variance, shows also a peak at quasi 60 days. The first mode of variability for K2 corresponds to 99% of total variance. The dominant mode of variability for K2, which is located in the NBUC core, aproximately 50 km from the coast, has the most variance at 14 days and also between 25 and 60 days.

Despite of the large variability observed in the NBUC at 5°S (SCHOTT et al., 1998) be related to equatorial processes, and not to the sSEC (STRAMMA et al., 2003), the large variability computed at 11°S is mostly influenced by the migration of the sSEC (SCHOTT et al., 2005).

According to Schott et al. (2005) the NBUC and NADW transports are not correlated. Therefore it appears that there are two different physical processes at work in the upper and lower layers. These authors claim that a possible reason for intraseasonal variance in the NADW domain has been identified as upstream instability from eddies passing into the DWBC.

The variance preserving spectrum of the PCAs for the moorings K1 to K5 show the main period band of most variance. K3 and K4 are located in the NADW. The first EOF mode in the K3 mooring (Table 2) is responsible for 63% of the variability and it is located at 100 m depth. A second mode corresponds to 34% of the total variability and it is centered between 300 and 500 m depth (Table 2).

The variance for K4 has a pronounced maximum located at 1900 m depth, approximately at the NADW core. The amplitude of this mode has a periodicity of 14-25 and 30-60 days (Figure 3.5d). The first maximum is about 30 days and the second maximum peak is 60 days, in agreement with Schott e al (2005).

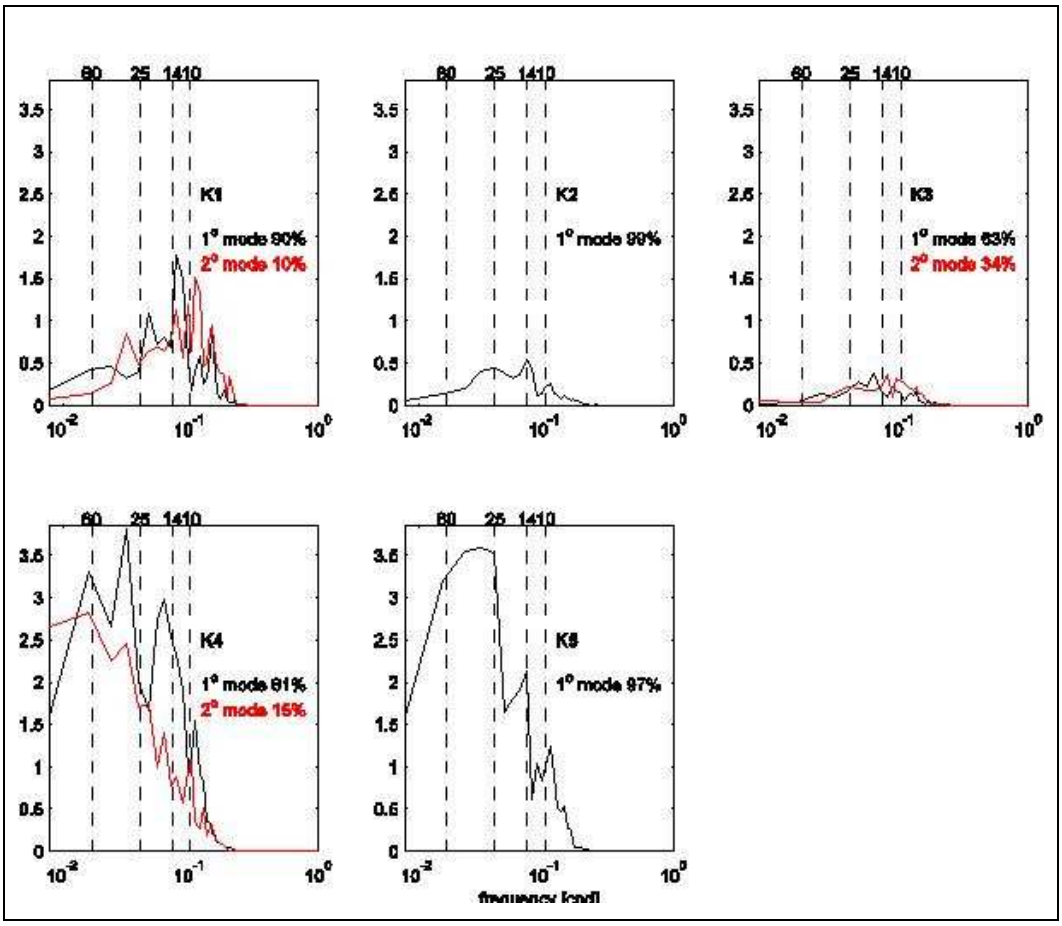

Figure 3.5 – Variance preserving spectrum of the first Principal Component for current in the: a) K1, b) K2, c) K3, d) K4 and e) K5 stations.

On the other hand, the second EOF mode (Figure 3.5d), in K4 station, is responsible for 15% of the variance (Table 2) at 500 m depth. The first maximum of this EOF corresponds to a periodicity of 30 and 60 days. In this position, below the STC level, Schott et al. (2005) found a substantial and persistent recirculation offshore from the NBUC along 5°-11°S. Particularly at 500 m depth, at 11°S, they found a statistically significantly southward current with approximately 6.8 cm s^{-1}. This counterflow suggests an offshore band of intermediate water recirculation in this latitude range, up to 5 Sv and reaching down to NADW densities.

There are some possible explanations for the origin of this flow. One would be the deflection of zonal currents. Northwest of the 5°S section (Figure 3.1c), there is a westward flow across the 35°W section (SCHOTT et al., 2005). In the opposite direction there is an eastward flow by the South Equatorial Underurrent (SEUC) at 150-400 m depth, between 2.5° – 4°S, and the Southern Intermediate Countercurrent (SICC) at 1.5° – 3.5°S, reaching 500-1200 m depth. However, no evidence of a southward deflection has been reported for these currents, because the SICC and SEUC transport stays nearly constant until 28°W section. The other would be an inflow from the east as part of the deep SEC, which gets deflected southward before reaching the Brazil coast and thus, forms an offshore counterflow to the deep NBUC. Also, it could be explained by a retroflection of the deep NBUC just a little bit north of the northeastern tip of Brazil, to supply the southward offshore flow across 5°S.

However, we found two options in the analysis of results obtained from SODA reanalysis and in the numerical results from ROMS model (1/12°). These results are explained in the ROMS and SODA results. In the calculation of the EOF analisys for two coupled fields, temperature and current measurements for the same time interval (see Table 2) were used for each K3 and K4 stations and the results are summarized in the

Table 3.

Table 3 – EOF analysis applied to the (coupled field) Meridional current-Temperature along transect 11°S. The coupled field analysis for current and temperature for K1 and K4 mooring data field. CC is the correlation coefficient, which quantifies the strength of the coupling.

Mooring	*EOF Mode*	*SCF (%)*	*CC*	*Period (days)*		*Depth (m)*
				Velocity	*Temperature*	
K3	1°	99	0.60	61	61	1885
K4	1°	98	0.34	67	67	1906

The Correlation Coefficient, the strength of the coupling, was computed giving a value of 0.60 (CC varies from 0 to 1). The coupled fields' analysis shows, through Principal Component Analysis, a stronger coupling for the temperature and the velocity of K3 at about 2000 m depth. The temperature is strongly coupled to the current of the mass of water at this depth. On the other hand, in K4, the coupling between the temperature and the current fields is not as strong as in K3, with a CC value of 0.34. The periodicity of the projection of the coupled fields onto the current and the temperature values agree with the single field analysis.

In the Principal Component Analysis of the EOF1 for the temperature and current for K3, from March 2000 to September 2001, there is a distinctive trend for a stronger coupling, mainly in the first 12 months of data, from March 2000 to February 2001. The PCA for temperature and current are synchronized each quasi-two months, where there is a trend for more variance at the same time for the two fields. More time of PC analysis is needed to conclude if this EOF1, which represents the core of the NADW as part of the MOC of the Atlantic, is an area of quasi-permanent coupling of temperature and current. This knowledge will allow estimations of the current field contribution to the interhemispheric heat transport at this level. This depth is at the axis of the DWBC, which carry the NADW southward accomplished by migrating anticyclonic eddies. These eddies present a 60-70 days variability (DENGLER et al., 2004), according with the results found here (Table 3). The DWBC break up into a series of anticyclonic eddies, denoted by their positive bowl-shaped temperature anomaly. This bowl-shaped temperature shows that more high temperatures are concentrate into eddies at the DWBC level. It shows a strong coupling between high velocities from eddies and temperatures anomalies inside them.

Meridional variability and depth dependence of the horizontal fields

The seasonal variations of the winds are associated with the north-south movements of the Intertropical Convergence Zone (ITCZ), the band of cloudiness and heavy rains where the southeast and the northeast trades meet. The southeast trades are most intense and penetrate into the north hemisphere during the northern summer when the ITCZ is between 10° and 15°N. During those months the surface currents are particularly strong. The NBC, after crossing the equator, change direction sharply eastward to feed the North Equatorial Countercurrent. The Equatorial Undercurrent is also strongest during this season when the east-west slope of the equatorial thermocline is at maximum (STRAMMA and SCHOTT, 1999; LUMPKIN and GARZOLI, 2005).

The ITCZ reaches its southernmost latitude in March and April, bringing a rainy season to northeastern Brazil. In some years the rains fail, and such years of drought. The droughts characteristically occur when the South Atlantic subtropical high expands equatorward and the ITCZ moves farther north. During those periods, the South Atlantic

trade winds become stronger than normal and anomalously cold surface water appears in much of the equatorial Atlantic. The tropical Atlantic experiences annual changes in SST of 6° - 8° C that are substantially greater than the interannual (Peterson and Stramma, 1991).

The SST variations in the tropical Atlantic play an important role modulating the climate variability, in particular over the adjacent continental regions (Kayano et al., 2005). This thermal gradient acts through the buoyancy forcing over the space-time variability of the high to low pressure areas in the atmosphere. In equatorial regions, the trade winds flow into the low pressure in the thermal equator, located more to northern hemisphere. Consequently, the near-surface winds of the tropical Atlantic are dominated by the southeast and northeast trade wind systems, which converge at the ITCZ. On the seasonal time scales the ITCZ migrates northward and southward and leads to changes in the upper ocean circulation.

The variation of the ITCZ over the seasonal cycle of surface currents is a response to the seasonally varying wind field. The ITCZ moves northward from boreal spring to summer and the zonal currents as the NEC and the SEC follow this northward displacement (PETERSON and STRAMMA, 1991; STRAMMA and SCHOTT, 1999; STRAMMA and ENGLAND, 1999). The dynamics that controls the migration of the sSEC bifurcation in the western boundary may be a result of the seasonal changes of the surface winds speed, which is in great part driven by SST seasonality. The analysis will focus on investigating the model responses to the monthly mean temperature conditions represented by Figure 3.6.

A seasonal meridional change in the SST along the South Atlantic western boundary can be observed (Figure 3.6). The high temperatures are from December to April, after these high SST values have been shifted northward, and warmer waters are only observed at the ocean area closer to the equator and limited to 8°S. This seasonal difference in SST fields creates a seasonal meridional temperature gradient along the south Atlantic, which drives the atmospheric general circulation that, in turn feedbacks the upper ocean layer circulation through wind stress.

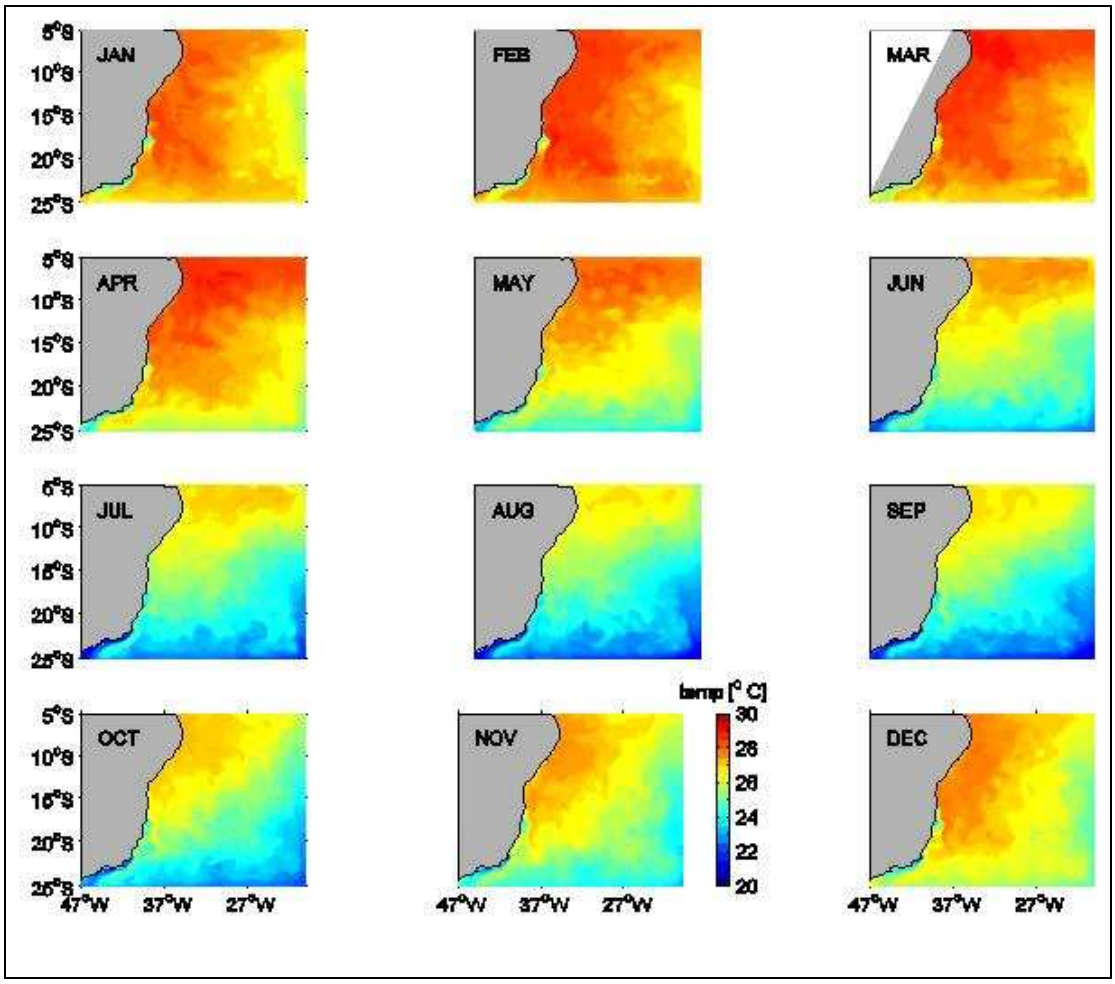

Figure 3.6 – Monthly mean distribution of SST obtained from the last year of a climatological simulation.

Model results show the mean monthly horizontal velocity fields during last year of simulation from ROMS. Monthly mean for three depths are showed in the Figures 3.7, 3.8 and 3.9, 100 m, 200 m and 500 m depth respectively.

At 100 m depth we can see little latitudinal variability where the currents are reversing (Figure 3.7). Many eddies along the coast mask the bifurcation of the sSEC. In the Figure 3.7 the simulation show that the sSEC reaches the Brazilian shelf between 13°S and 15°S, for April, May and June diverging into two western boundary currents; flowing to the north as North Brazil Undercurrent – NBUC, and to the south as the Brazil Current – BC (STRAMMA and ENGLAND, 1999; Stramma et al., 2005; Schott et al., 2005). For the months October, November and December the meridional component is reverse about 12°S. These results at 100m depth corroborate with the work of Rodrigues et al.(2007), where a bifurcation at surface was found between 10° and 14°S near the surface.

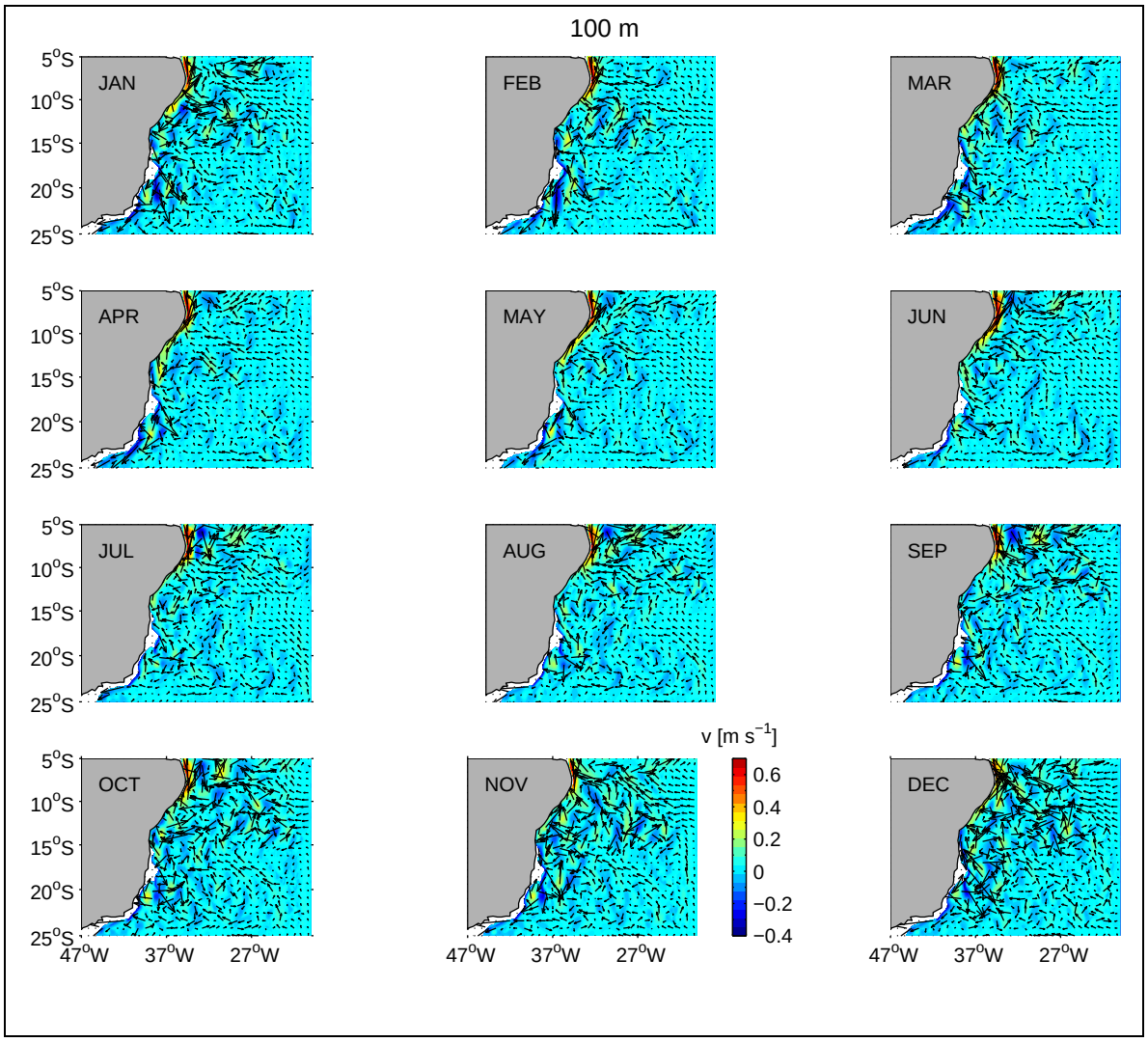

Figure 3.7 – Monthly mean horizontal current fields at 100 m depth obtained from last year of a climatological simulation.

At 200 m depth is approximately the core of the NBUC level (SCHOTT et al., 2005) and the lower limit of the CW, respectively. An analysis for 200 m depth, for November and December, (Figure 3.8) the positive meridional component of velocity is as a continuous current reaching about 13°S. For the months May and June the current is reverse between 17°-20°S, and the flow southward representing the BC has a behavior like an eddy. This eddy characteristic is typical of this area. Between 20°S and 31°S the continuous Brazil Current is associated with eddies and meanders (SCHMID et al., 1995). About 20°S close the Vitoria City and north of Cabo Frio, a complex topography at 90 degree angle of the Brazilian coast influences the BC. This topographic characteristic is named Vitória Trindade Ridge. The position of the BC changes considerably with time. Sometimes the greater part of the BC turns eastward, north of the Vitória Trindade Ridge, and then turns back to the west close to coast. At other times, a large part of the BC flows through the western channel of the Vitória Trindade Ridge. The hypothesis is that the translation of this eddy is strongly influenced by the local topography. This complex topography contributes to mask the bifurcation of the sSEC at this region. The vortices form a northward flow attached to coast associated to NBUC and at east a southward flow linked to BC.

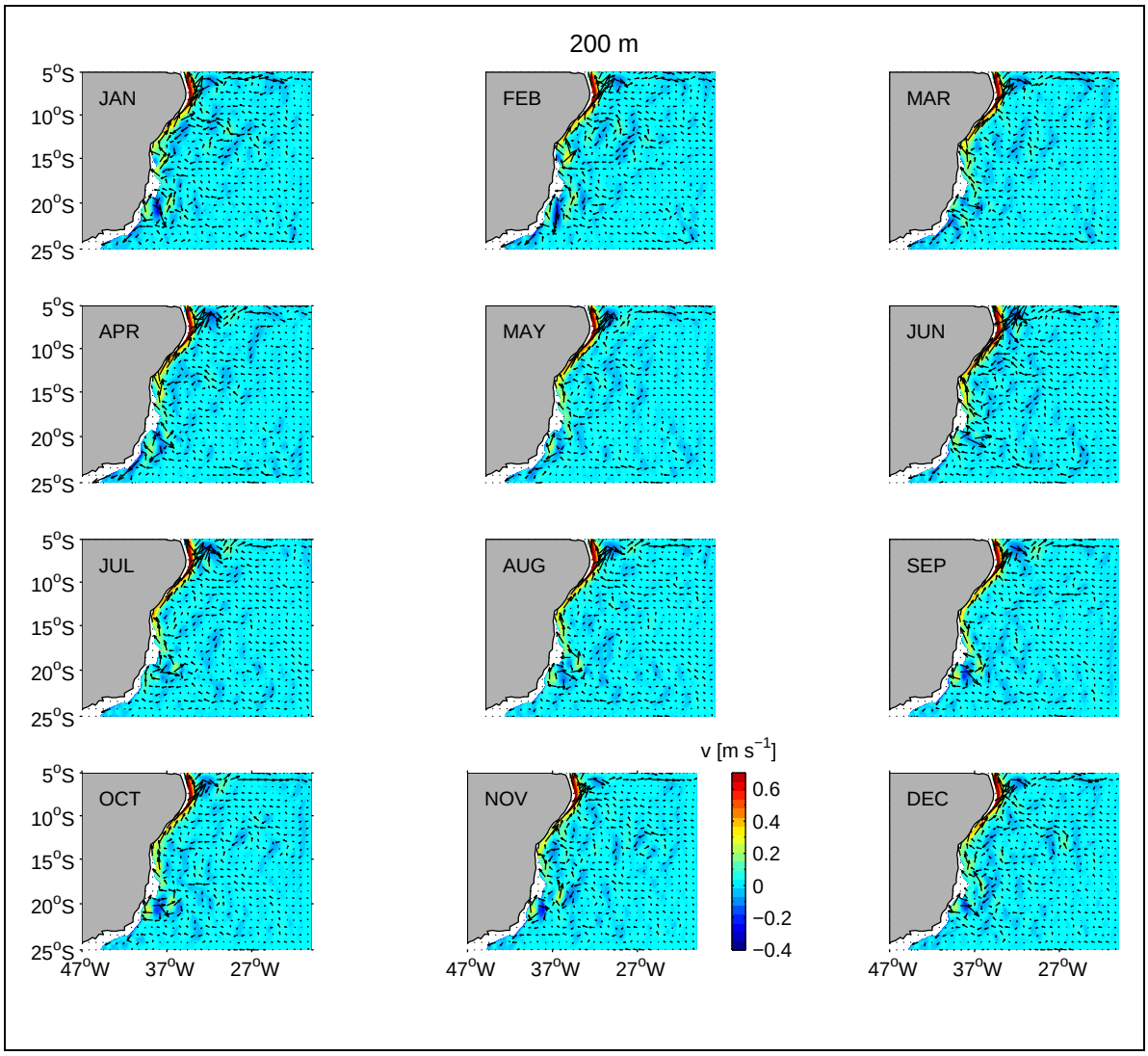

Figure 3.8 — Monthly mean horizontal current fields at 200 m depth obtained from last year of a climatological simulation

The northward extension of the subtropical gyre reduces with increasing depth, while the tropical cyclonic gyre progresses southward as wedging of the thermocline in the equatorward side of the subtropical gyre, and reflects a poleward shift with depth of the subtropical gyre. According with Stramma and England (1999) the northern limb of the gyre, or the sSEC in the near-surface layer, reaches the shelf of Brazil near 16°S and separates into the southward flow of the Brazil Current and at subsurface into the northward flow of the NBUC while in the Central Water layer the sSEC reaches the Brazilian continent at about 20°S and in the AAIW the sSEC reaches the shelf at about 26°S.

Cirano et al. (2006) found a depth dependence of the sSEC bifurcation; they used the OCCAM from Ocean Circulation and Climate Advanced Modeling Project. Their results indicate that the model is capable of representing the southward zonal migration of the sSEC with the increase of depth. The sSEC bifurcation was found to be between 9°S – 15°S at level of the TW, at 25°S at level of the SACW and a bifurcation between 25°S – 30°S at level of the AAIW. Rodrigues et al., (2007) used a reduced-gravity, primitive equation OGCM to investigate the seasonal variability of the bifurcation of the sSEC. The found that the annual mean meridional velocity averaged within a 2° longitude band off the South American coast shows a depth dependence of the sSEC bifurcation. It occurs at about 10° – 14°S near the surface, shifting poleward with increasing depth, reaching 27°S at 1000 m.

According with Stramma and England (1999) and Stramma et al. (1995) the sSEC in the near-surface layer reaches the shelf near 16°S and separates into the southward flow of the BC and at subsurface depth into the northward flow of the NBUC. The tropical cyclonic gyre progresses southward as lower depths, which can be understood as wedging of the thermocline in the equatorward side of the subtropical gyre, and reflects a poleward shift with depth of the subtropical gyre. The upper ocean in the subtropical South Atlantic is governed by the subtropical gyre with a southward shift of the northern part of the gyre, the tropical circulation shows several depth-dependence zonal current bands. The present work not only suggests a seasonal variability on the local of the sSEC divergence, but also indicates its depth dependence. According to the model results, the sSEC bifurcation shifts southward as ocean depth increases. For example, it varies from 12°S at 100 m depth to 20°S at the 500 m depth (Figure 3.9). These results corroborate some recent works such as Cirano et al. (2006) and Rodrigues et al. (2007) and confirm that the ROMS model can represent the dynamic of the western boundary of the South Atlantic.

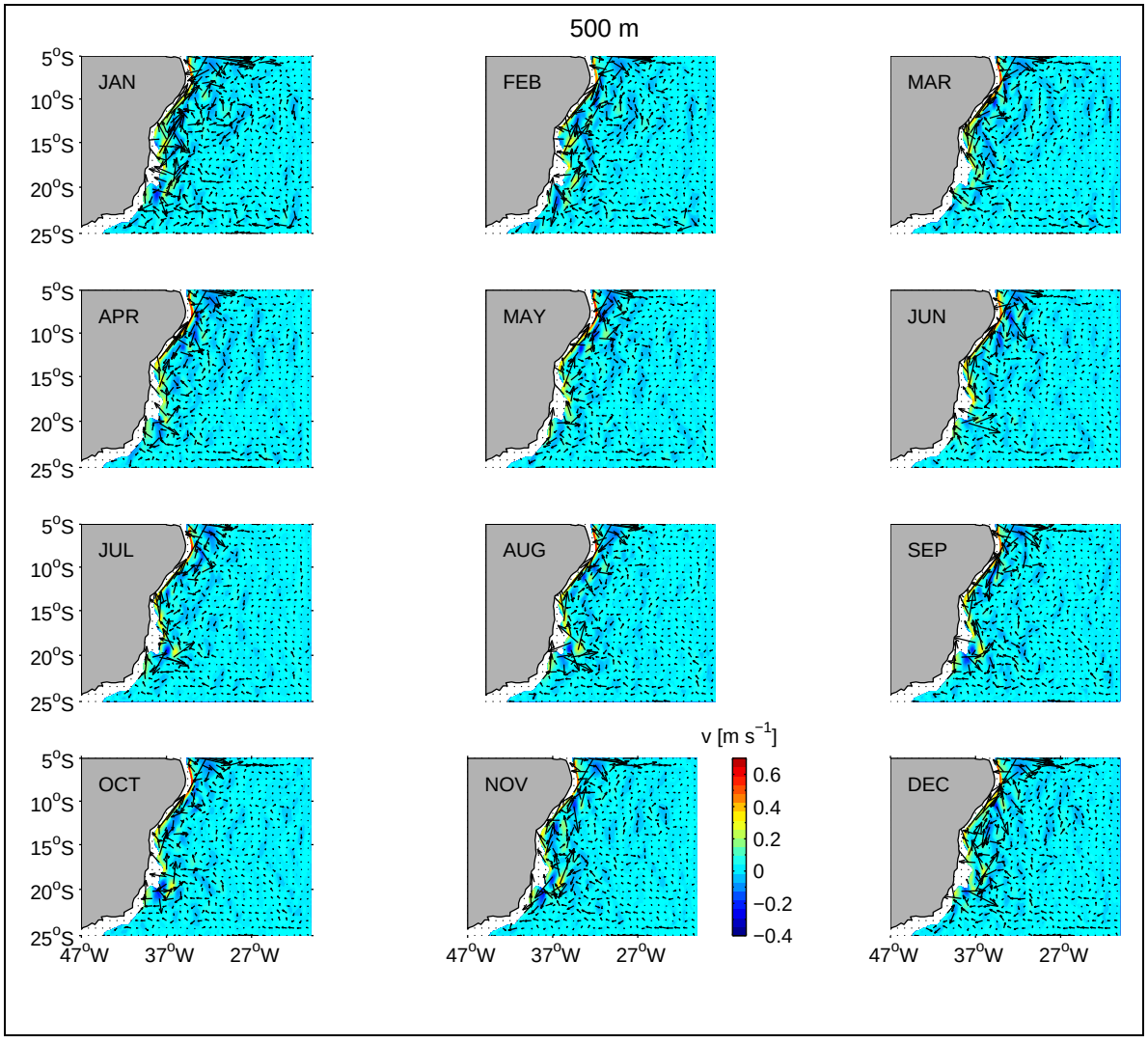

Figure 3.9 – Monthly mean horizontal current fields at 500 m depth obtained from last year of a climatological simulation.

The bifurcation of the SEC is defined here as where the meridional transport from the continental slope is zero. In the Figure 3.10 a mean alongshore velocity averaged within a 1° longitude band off the South American coast shows that the sSEC bifurcation occurs southernmost at 19°S in May-June and northernmost at 13°S in November and December. This result restricts the analysis close to coast and the average within 1 degree from the coast reduces the influences of the vortices showed in the Figures 3.7 to

3.9. Additionally, we can see that when the bifurcation is southward the NBUC is stronger. At the same time, as when the bifurcation is northward the NBUC is weaker, this confirms the results in Rodrigues et al. (2007). Moreover, according with Schott et al. (2005) the seasonal cycle of the NUBC presents the main northward maximum is in July and minimum in October-November.

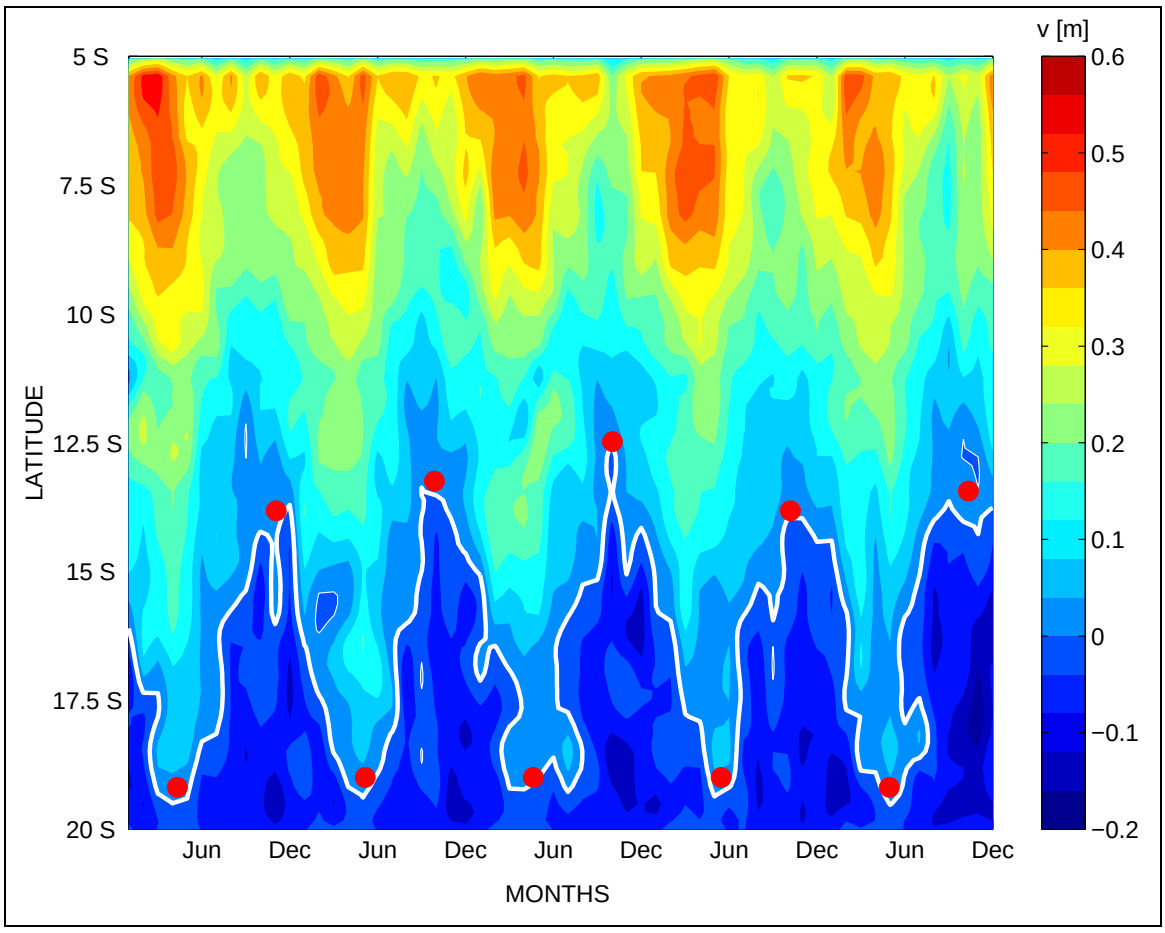

Figure 3.10 – Hovmöller of the meridional component of velocity at 200 m depth (m s^{-1}). Results from the last 5 year of simulation of ROMS Model. The alongshore component is a mean of one degree of longitude from the coast. The white line represent where the western boundary currents are reverse.

Current structure and transport variability

The total NBUC transport at 11°S accounts for 25.7 Sv and is about equal to its transport at 5°S (SCHOTT et al., 2005). The NBUC is fully established at 11°S; consequently the sSEC bifurcation is located south of 11°S. The NBUC transport anomaly time series shows strong fluctuations with amplitudes of about ± 15 Sv. Mostly fluctuations with bimonthly periods are dominant within the NBUC. The combined annual and semiannual harmonics cycle result in a maximal northward NBUC transport in austral winter with minimum in October and November.

The transport sections presented here contribute to infer about the level of coupling between the seasonal cycle of the NBUC and the alongshore intrannual variability of the sSEC bifurcation. According with Rodrigues et al. (2007) it is expected that, when the sSEC bifurcation is located more southward, the NBUC transport will be more intense. In opposition, when the sSEC bifurcation is displaced northward, the NBUC transport will be weaker. This reasoning is based on the fact that the inflow of the sSEC into the western equatorial regime feeds the NBUC mainly in the depth range of the Central Water Layer (100 – 500 m). As a consequence the seasonal migration of the sSEC could be

responsible for the NBUC transport seasonality (SCHOTT et al., 2005).

Mean alongshore transport values obtained from ROMS simulation at 11°S are presented for November and July, respectively (Figures 3.11 and 3.12). The isopycnal σ_θ = 24.5 kg.m^{-3} separates the upper TSW from the upper thermocline waters, and the σ_Θ = 26.8 kg.m^{-3} the lower level of the water supplying the Equatorial Undercurrent (EUC) (SCHOTT et al., 1998). In the upper ocean of the tropical and subtropical Atlantic the SACW is observed, which shows a nearly T-S relationship. The SACW is warm and salty compared to the AAIW located underneath.

The isopycnal σ_θ = 27.1 kg.m^{-3} in the tropics marks the transition between the SACW and the AAIW (STRAMMA and ENGLAND, 1999). The AAIW can be recognized by a subsurface oxygen maximum and a salinity minimum (Figure 1 in STRAMMA and ENGLAND, 1999). The mean flow field of the AAIW indicates that the northern limb of the sSEC at this water mass reaches the shelf at about 23°S and turns northward while the stronger westward component within the BC recirculation cell reaches the shelf near 28°S and turns southward.

The isopycnal σ_θ = 32.15 kg.m^{-3}, about 1100 m depth, indicates the lower boundary of the upper warmer waters, as well as the lower boundary of the AAIW (Figures 3.11 and 3.12). This is the layer where most of the northward NBUC transport occurs. Bellow 1200 m depth we found the NADW extending to about 4000 m depth (σ_θ = 45.9 kg.m^{-3}). This is the place where the DWBC acts transporting cold waters from the North hemisphere with a net transport southward (see Figure 3.1c and Figures 3.11-3.12). The NADW is located underneath upper Circumpolar Deep Water (uCDW), between about 1200 m depth and 3900 m depth in the tropics. The NADW is separated into three layers as upper, middle, and lower NADW, identified by a salinity maximum for the upper NADW and two oxygen maximum for the middle and lower NADW. The shallowest part of the upper NADW shows a salinity maximum that is correlated to elevated concentrations of tritium and chlorofluorocarbons (RHEIN and STRAMMA, 2005). The salinity maximum lies near 1600 m depth near the equator and near 2500 m depth at 25°S. The deep range influenced by the NADW decreases varies from about 1200 to 3900 m near the equator and 1700 to 3000 m depth in the confluence zone of the Brazil and Falkland currents.

In the Figure 3.11 and 3.12 the ROMS results show the uCDW restricted to the isopycnals σ_θ = 32.15 kg.m^{-3} and σ_θ = 45.9 kg.m^{-3}. This isopycnal of σ_θ = 45.9 kg.m^{-3} separates the lower NADW from the northward spreading Antarctic Bottom Water (AABW), near the equator such as in Stramma and England (1999), Stramma and Peterson (1990). While near the SAC the potential density surface σ_θ = 45.87 kg.m^{-3} marks the NADW/AABW boundary.

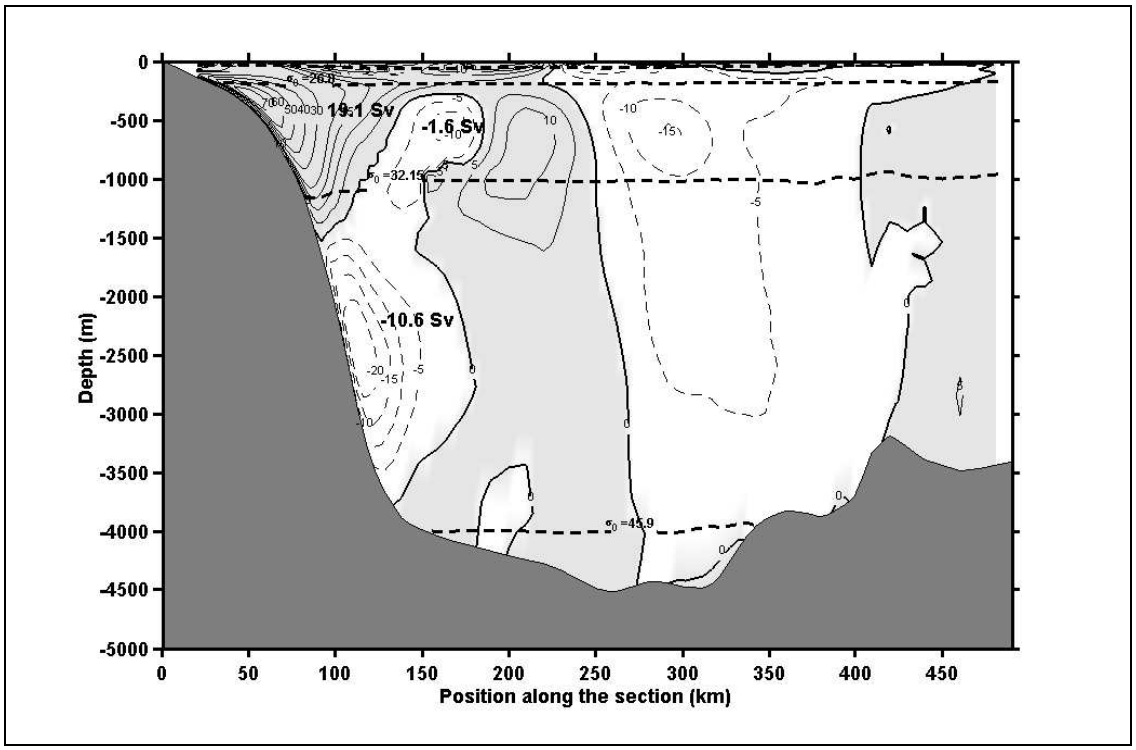

Figure 3.11 – Meridional transport obtained from ROMS simulation at 11°S: November. Positive values are indicated by solid lines corresponding to northward currents, while southward transport is indicated by dashed sections. Horizontal dashed lines indicate the boundaries between different water masses.

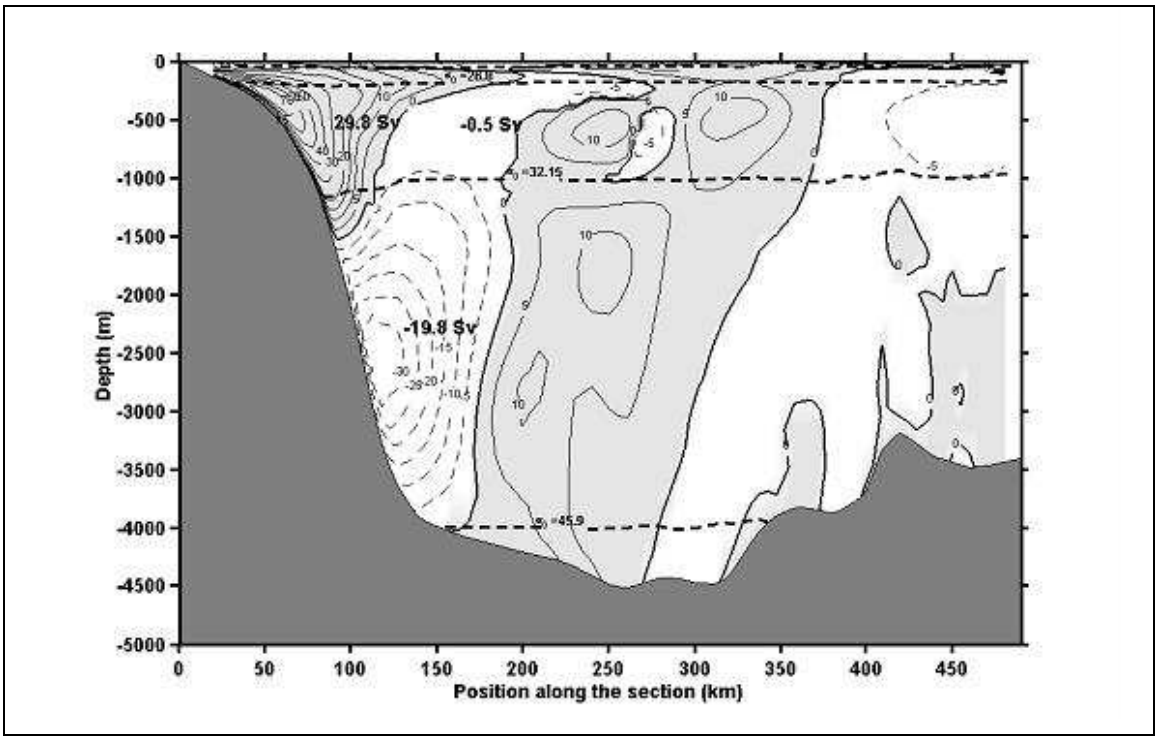

Figure 3.12 – Meridional transport obtained from ROMS simulation at 11°S: July. Positive values are indicated by solid lines corresponding to northward currents, while southward transport is indicated by dashed sections. Horizontal dashed lines indicate the boundaries between different water masses.

The northward NBUC with its core situated about 50 km from the coast, and at 180-250 m depth, where the transport is stronger, has been also detected from field measurements (SCHOTT et al., 2002; STRAMMA et al., 2003; SCHOTT et al., 2005). Toward the surface the velocities decrease considerably, confirming the undercurrent characteristic of the NBUC. Still, in the upper layers, it is observed from model transects, the presence of a mean southward flow at 300-900 m offshore to the NBUC (about 150 km from the coast). This southward flow was evidenced from field measurements (SCHOTT et al., 2005), as well as in the present numerical results and through PCA of the field data.

From ROMS simulations, this counterflow is well formed just offshore of the NBUC at 11°S. The climatological modeling results indicate a stronger northward transport of the NBUC during the austral winter of 29.2 Sv with, approximately, the same magnitude of the moorings data registered for austral winter in the (27.7 Sv). Furthermore, during austral summer, less accentuated northward transport is verified from the model results (20.8 Sv) and field measurements (22.7 Sv). It is suggested that there is a link between the strength of NBUC transport and the latitude where the sSEC bifurcates near the Brazilian edge at 200 m depth. When the sSEC bifurcation is southward, during austral winter, the NBUC transport is stronger.

Model results indicate that the NBUC at 11°S presents an almost steady flow, reaching down to about 900 m depth, with a slower transport during austral summer (November) and a slightly higher northward transport in winter (July). These same features are observed at the experimental transects obtained from moorings data. Mean annual northward NBUC transport calculated from model is 23.4 Sv. This value is in good agreement with the 25.4 Sv estimated by Schott et al. (2005). The K1-K2 moorings data indicate the presence of the NBUC core in July at about 190 m depth and higher velocities of about 70 cm s^{-1}. The November measurements indicate a NBUC core at 200 m depth, with velocities reaching 35 cm s^{-1} at that latitude. Model results to November show a subsurface NBUC core situated at about 250 m depth, and velocities of up to 70 cm s^{-1}. In July, the numerical NBUC core is situated close to 300 m depth, with maximum velocities of about 72 cm s^{-1}, which is in good agreement with values encountered by Schott et al. (2005).

The current structure obtained from ROMS in a section at 11° S (Figure 3.13) is representative of the alongshore current measurements from the moorings section (represented in Figure 3.1c). Climatological monthly mean of ROMS simulation are represented in the Figure 3.13, where we can see the temporal evolution for the alongshore component. The core of the NBUC is well formed at this latitude, and the maximum alongshore currents reaches 0.7 m s^{-1} as in Schott et al. (2005). The higher values of the DWBC from measurements are found in a mean section for June, July and August, where the DWBC is more defined and attached to coast. In the results from ROMS the DWBC is more defined and stronger as other months in July and August.

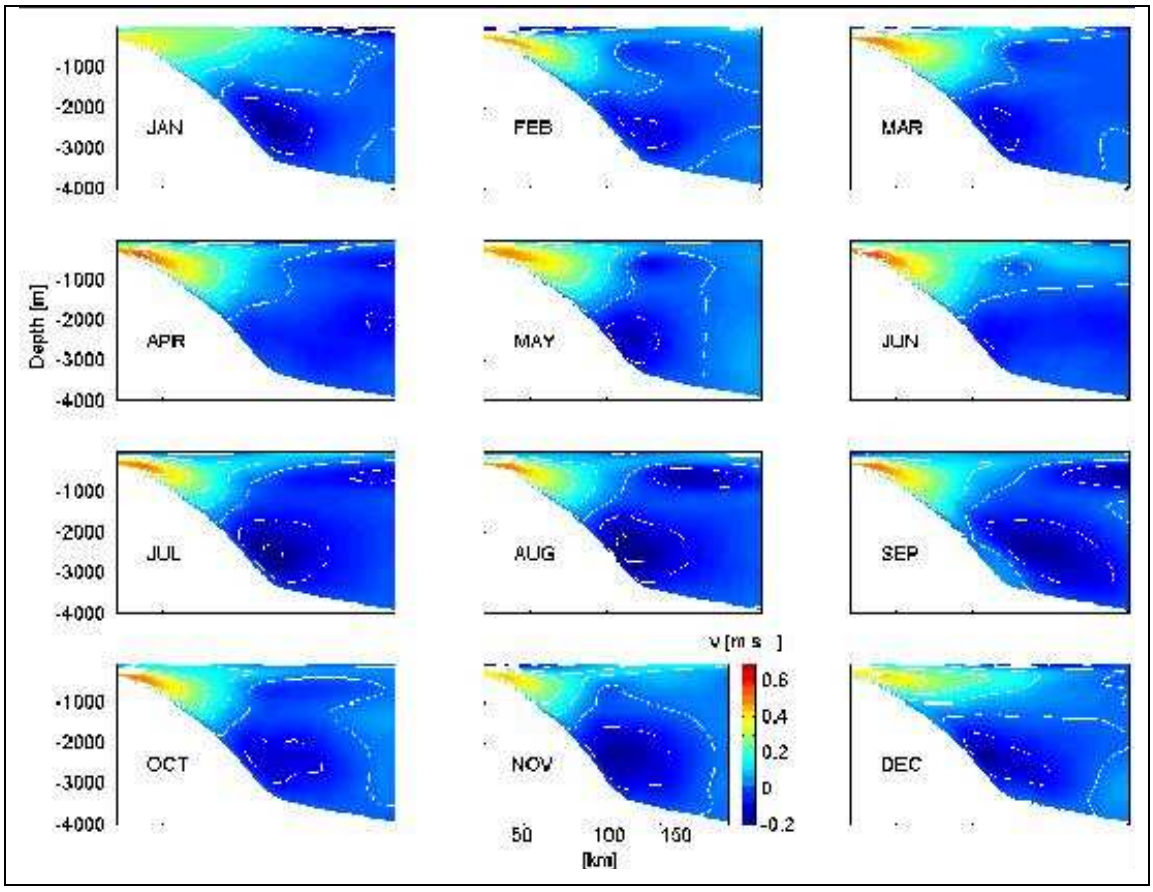

Figure 3.13 Alongshore monthly mean velocities obtained from last year of the ROMS simulation Section at 11°S. Positive values are indicated by solid lines corresponding to northward currents, while southward flow is indicated by dashed sections.

Climatology of the SODA reanalysis

A monthly mean of the alongshore current for 47 years of SODA reanalysis is analyzed to identify the bifurcation of the sSEC. The area covered here is from 20°S to 5°S and from 41°W to 30°W. Such as in ROMS results (Figures 3.7, 3.8 and 3.9) the alongshore current fields of SODA reanalysis in the Figures 3.14 and 3.15, the bifurcation latitude of the sSEC is defined as the place where the western boundary currents are reverse. Here is chosen the bifurcation where the alongshore component of the velocity is zero, the null dashed line attached to coast. At 200 m depth, the northernmost position where the alongshore currents are reverse occurs in December and January at about 13°S. The southernmost position occurs in from May to July at about 17°S (Figure 3.14).

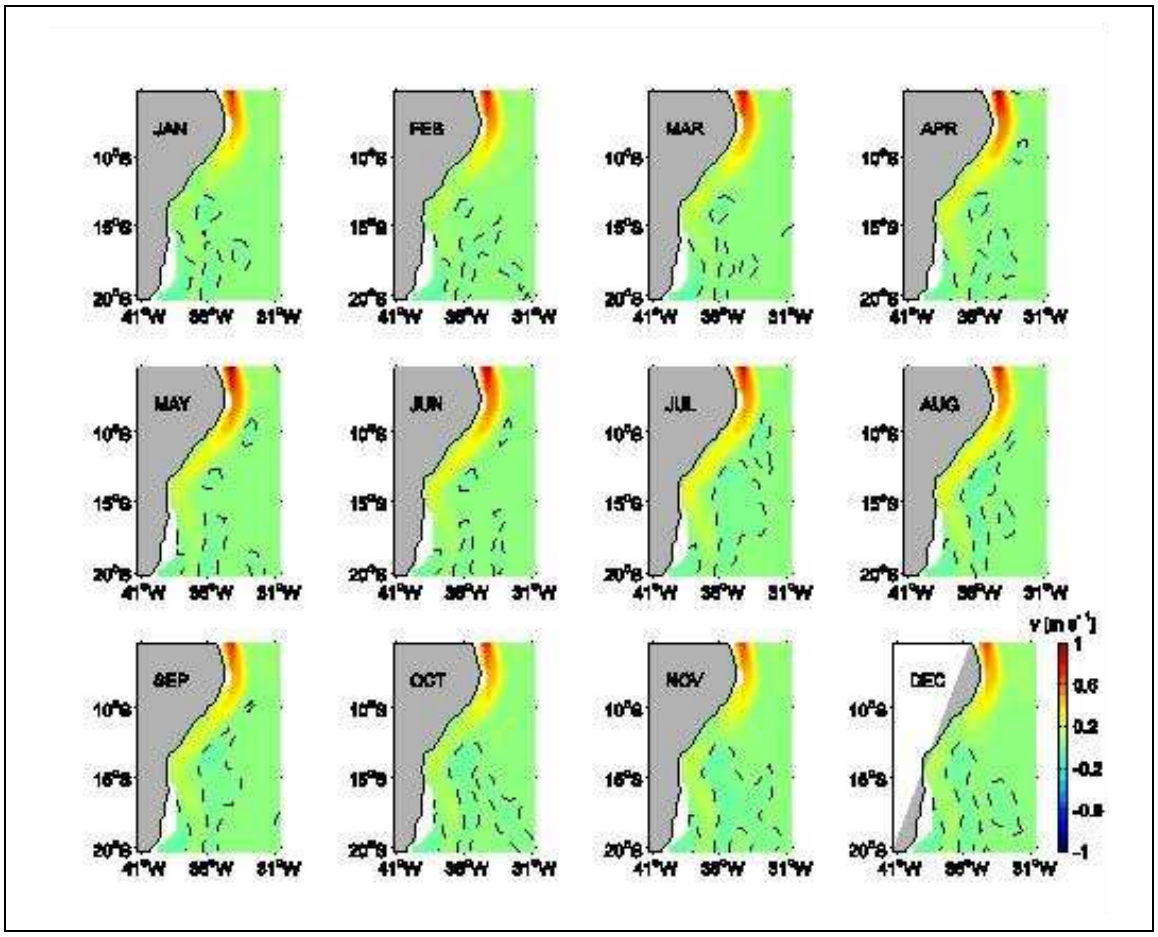

Figure 3.14. Monthly mean horizontal current fields at 200 m depth obtained from 47 years of the SODA reanalysis.

According to profiles from ROMS, the results from SODA were also analyzed in a horizontal section at 500 m depth (Figure 3.15). The alongshore current are reverse northernmost at about 17°S in October and November while the southernmost reverse of currents is from March to July at about 19°S. These fields are important to confirm the depth dependence of the bifurcation of the sSEC, as such as in Rodrigues et al. (2007) and Cirano et al. (2006), as well in ROMS model results in this work (Figures 3.7, 3.8 and 3.9).

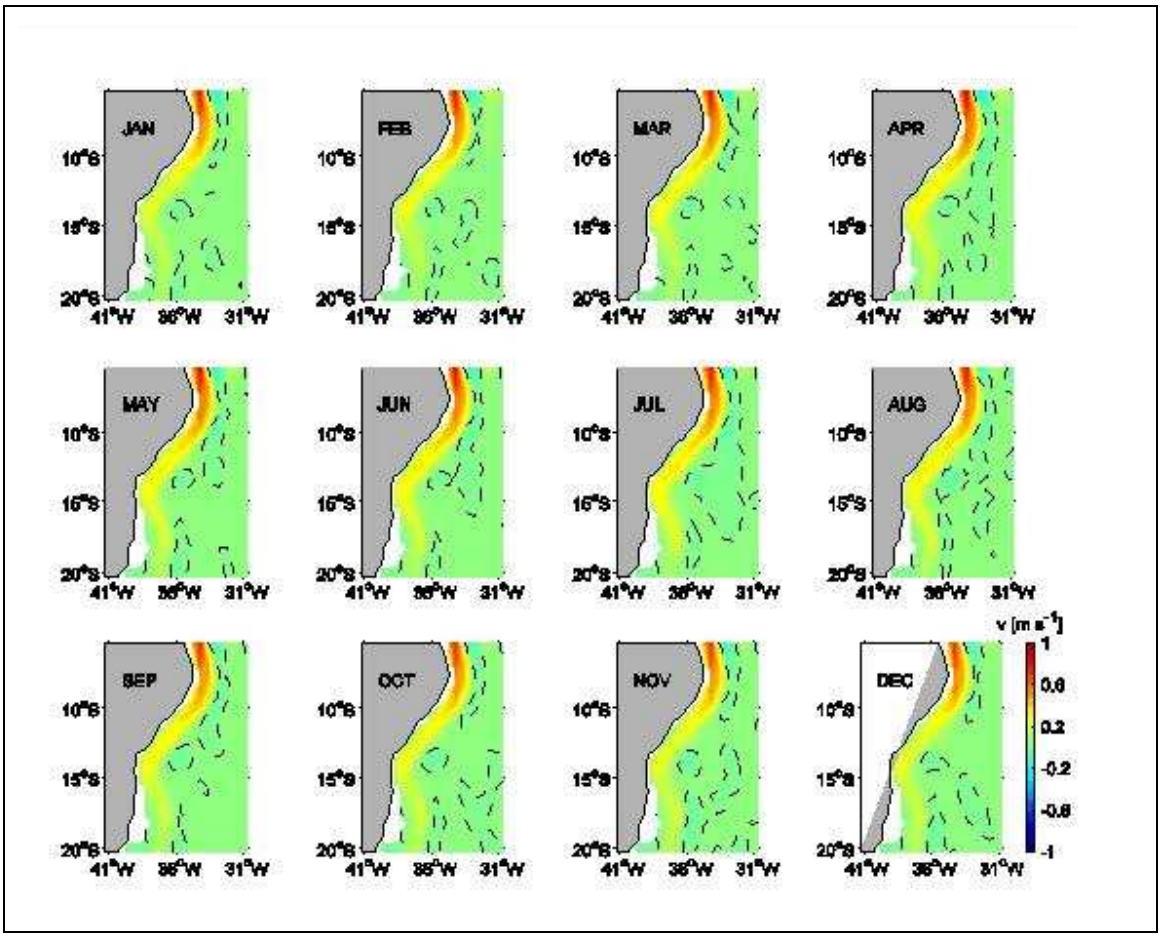

Figure 3.15 – Monthly mean horizontal current fields at 500 m depth obtained from 47 years of the SODA reanalysis.

Such as in ROMS results, the bifurcation of the sSEC is defined here as where the meridional transport from the continental slope is zero. In the Figure 3.16 mean alongshore velocity averaged within a 1° longitude band off the South American coast for 5 years is showed. From SODA results, the seasonal variability of the sSEC doesn't follow the same pattern each year. Then, a low pass filter for 90 days was applied to eliminate the intraseasonal variability, which masks the seasonal pattern of variability. The result here shows an interannual variability of the bifurcation of the sSEC. The main variability is each about 2 years. The question here is what causes this interannual variability.

Witter and Gordon (1999) found interannual variations from empirical orthogonal functions of TOPEX/POSEIDON sea level observations. Two main modes of variability were identified. The dominant mode of basin-scale zonal wind has the same temporal signature, suggesting a link between the observed variation of gyre-scale circulation and the regional wind forcing. Time variations of this mode also coincide with a transition from a broad Agulhas eddy corridor. A second mode isolates interannual variations in the Brazil-Malvinas Confluence region. These interannual variations contribute significantly to the total South Atlantic variability. These variations may be related to interannual variations of the latitude of the sSEC bifurcation. In summary, it can be said that this work point out an interannual variability of the sSEC bifurcation. A full description, however, would require a considerable effort on the characterization of the Agulhas eddy phenomenon and a correlation with the sSEC bifurcation.

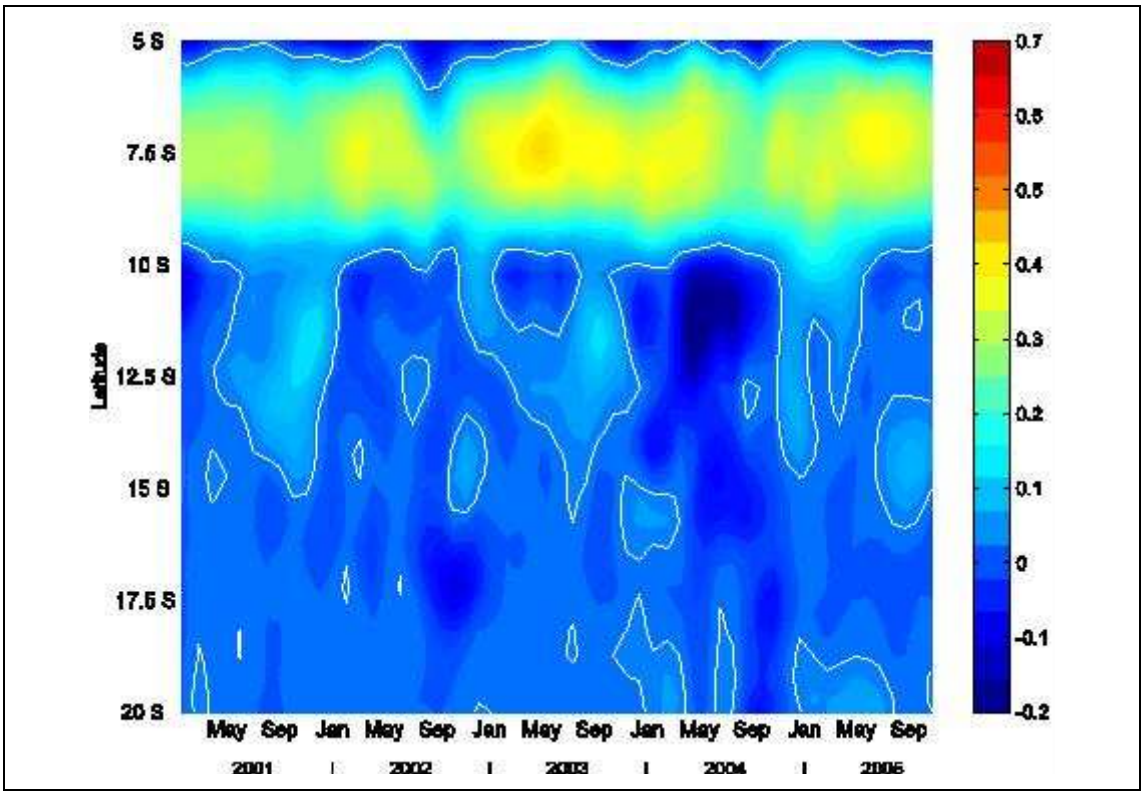

Figure 3.16 – Hovmöller of the meridional component of velocity at 200 m depth, for 2001 to 2005. Three months low pass filtered data were used. The alongshore component is a mean of one degree of longitude from the coast. The white line represent where the western boundary currents are reverse.

4. CONCLUSION

The main motivation behind of this study was to investigate the presence and the dynamic of the southern band of the South Equatorial Current (sSEC) as well as the vertical structures in the western Atlantic Ocean boundary comprised within 5° S - 25° S and 20° W - 47° W. These coordinates limits the area where the sSEC encounters the South American continent and bifurcates, with the water flowing north and south as two western boundary currents, the NBUC and the BC, respectively. This is a region of complex links between climatic variability of the SST and heat content of the upper layers of the tropical Atlantic, atmospheric convective systems and precipitation on the adjacent continent, especially on the Brazilian Northeast region. We are particularly interested on evaluating the capacity of a specific numerical modeling technique on reproducing seasonal transfers of heat and oceanic mass between different sectors of the subsurface tropical Atlantic and identify the temporal scales of occurrence of these phenomena.

Numerical transports and currents results were compared to ocean measurements obtained from moorings data deployed at 11°S by the German part of CLIVAR program, from March 2000 to August 2004. These comparisons suggest that the climatological modeling approach employed here reproduces the main features of the circulation observed from field measurements. For example, numerical currents and transports distributions along water depth are similar to CLIVAR measurements. An important characteristic found in the simulated sSEC divergence is that it shifts southward as ocean depth increases: it varies from 12°S at 200 m depth to 19.5°S at the 500 m depth.

Model results show a strong northward under surface speeds up to 70 cm s^{-1} near 5°S, corresponding to the NBUC field data (STRAMMA et al., 2003). Despite of the larger variability observed at this latitude, the NBUC at 5°S has to be related to equatorial processes and not to sSEC variability (SCHOTT et al., 1998; STRAMMA et al., 2003).

Nevertheless the NBUC at 11°S can receive influences from seasonal migration of the sSEC. An important purpose of this study was to quantify the variability of the flow in the NBUC level, and to investigate if its dynamics is or not associated to the sSEC migration. The model simulations presented in this work stressed a seasonal migration of sSEC, with a southernmost shift at 19°S in May-June and northernmost at 13°S from September to January.

These periods correspond to the maximum (29.8 Sv) and minimum (19.1 Sv) northward NBUC transport at 11°S, respectively. The investigation of the K1/K2 moorings data through PCA confirmed the 14-25 days and a bimestral periodicity (50-300 m) of the NBUC core (EOF1 = 90 %). On the other hand, the NADW variability observed from moorings data K4 in deeper layers seems to be linked to upstream instability from eddies' passage in the DWBC. The PCA indicated a cycle of about 14-30-60 days (EOF1 = 81%) for the core of the DWBC at 1900 m depth.

According to simulations, the upstream DWBC between 7°S and 10°S is reinforced during austral winter (August), enhancing eddies generation. The anticyclonic structures reproduced in simulations shown a mean radius of 72 km and horizontal velocity of about 42 cm s^{-1} at 1900 m depth, which have the same order of magnitude of the average eddy scales estimated from moorings data (DENGLER et al., 2004). In opposition, the simulated upstream DWBC flow is clearly reduced during the austral summer (February), and less well defined eddies are present.

In the PC for a single field analysis, we also found in K4 at 500 m depth (Table 2) is 60 days of occurrence of maximum variance (EOF2=14%), where Schott et al. (2005) found a substantial and persistent recirculation offshore from the NBUC along 5° - 11° S. This counterflow suggests an offshore band of intermediate water recirculation in this latitude range, amounting to about 5 Sv and reaching down to NADW densities.

From ROMS simulations, we found this counterflow well formed just offshore of the NBUC at 11°S, with more intense flow in November and less intense in July, when was not found retroflection of the NBUC.

The results from SODA reanalysis were also analyzed in a horizontal section at 500 m depth. This analysis shows a counterflow off the NBUC from January to March, which reaches 10°S such as in Schott et al. (2005). From May to September this counterflow reaches higher latitudes, which suggest another contribution for the counterflow. This contribution is the westward flow from the deep cSEC shifting southward and feeding the counterflow.

The temporal evolution of the offshore counterflow to the NBUC suggests that this flow persist during the whole year. This phenomenon is important because it reduces the net heat transport toward the Northern Hemisphere. However, this counterflow still remains an open question, which needs to be confirmed by field data altogether with simulations north of 5°S.

The PCA for coupled fields shows not strong coupling in the first EOF at K4 station. However, the temperature is strongly coupled to the velocity current at the core of the DWBC for the first year of K3 mooring data, which reveals that these two fields are in the same phase each two months. There is a tendency for more variance at the same time for the two fields. The stronger coupling found here can be linked to the bowl-shaped temperature anomaly found Dengler et al., (2004), which shows that more highs temperatures are concentrate into the eddies at the DWBC level. It shows a strong coupling between high velocities from eddies and a high temperature into this eddies.

The results from SODA reanalysis reveal also an interannual variability of the sSEC bifurcation. These results could be associated to interannual variability in the Agulhas eddy corridor, which migrates into the South Atlantic Ocean in the form of an Agulhas ring. In summary, it can be said that this work point out the interannual variability of the sSEC as a key mechanism in the dynamics of the western boundary regime of the South Atlantic. A full description, however, would require a considerable effort on the modeling

of the interannual variability of the currents in the South Atlantic.

These results are very encouraging. This is the first time (to our knowledge) that a high-resolution (1/12^o) regional modeling approach is used for investigating the western tropical south Atlantic boundary and in particular the sSEC divergence area off Brazil. The ROMS seems to be able on reproducing the main features of the mean NBUC and NADW transports at different seasons near Brazilian edge. Numerical results were confirmed by moorings measurements and Principal Component Analysis, giving confidence in the simulated seasonal migration of the sSEC, which appears as a powerful justification to explain the seasonal cycle of the NBUC at 11°S. The verified model adjustment to offshore field data is promising. For example, these results can be extensively used in the future as boundary conditions for smaller-scale shelf sea modeling as a way to evaluate the remote influences of the open ocean forcing over the dynamics of the still little studied coastal seas neighboring the northeastern Brazilian region.

ACKNOWLEDGEMENTS

The authors thank the scientific team of the German Climate Variability and Predictability (CLIVAR) program and, in particular, our colleagues from IfM-GEOMAR for providing free access to the K1-K4 mooring data. D.V. also wishes to thank CAPES/DAAD (Coordination for the Improvement of Higher Education Staff/Deutscher Akademischer Austauschdienst) for scholarship support. R.M. acknowledges financial support from the Pernambuco State Agency FACEPE. This work was carried out under the CNPq Project "Variabilidade Biogeoquímica no Atlântico Tropical ao largo do Nordeste do Brasil - BIO-NE", Process 558143/2009-1.

REFERENCES

BOURLÈS, B.; MOLINARI, R. L.; JONHS, E.; WILSON, W. D.; LEAMAN, K. D. Upper layer currents in the western tropical North Atlantic. **Journal of Geophysical Research,** v. 104, p. 1361-1375, 1999.

CAMPOS, E. J. D.; GONÇALVES, J. E.; IKEDA, Y. Water Mass Characteristics and Geostrophic Circulation in the South Brazil Bight - Summer of 1991. **Journal of Geophysical Research**, v. 100, n. 9, p. 18537-18550, 1995.

CIRANO, M.; MATA, M. M.; CAMPOS, E. J. D, DEIRÓ, N. F. R. A Circulação oceânica de larga-escala na região oeste do Atlântico Sul com base no modelo de circulação global OCCAM. **Brazilian Journal of Geophysics**, v. 24, n. 2, p. 209-230, 2006.

Da SILVA, A. M.; YOUNG, C. C.; LEVITUS, S. Atlas of surface marine data 1994, vol. 1, algotithms and procedures, NOAA Atlas Nesdis 6. US Department of Commerce, NOAA, **Nesdis**, Usa, 74p. 1994.

DEFANT, A. Die absolute Topographie des physikalischen Meeresniveaus un der Druckflächen, sowie die Wasserbewegungen im Raum des Atlantischen Ozean. Wissenschaftliche Ergebnisse Deutschen Atlantischen Expedition auf dem Forschungs und Vermessungsschiff. "**Meteor**", 1925-1927, v. 6, n. 2, p. 191-260, 1941.

DENGLER, M.; SCHOTT, F. A.; EDEN, C.; BRANDT, P.; FISCHER, J.; ZANTOPP, R. Break-up of the Atlantic deep western boundary current into eddies at 8°S. **Nature** v. 432, p. 1018-1020. 2004.

GORDON, A. L. Interocean exchange of thermocline water. **Journal of Geophysical Research**, v. 91, p. 5013-5046, 1986.

HAIDVOGEL, D. B.; ARANGO, H. G.; HEDSTROM, K.; BECKMANN, A. Malanotte-Rizzoli, P., Shchepetkin, A. F. Model evaluation experiments in the North Atlantic basin: simulations in nonlinear terrain-following coordinates. **Dynamics of the Atmosphere and Oceans**. v. 32, p. 239-281, 2000.

JOLLIFFE, I. T. **Principal component analysis.** Springer. New York. 2002

KAYANO, M. T.; RAO, V. B.; ANDREOLI, R. V. A review of short-term climate variability

mechanisms. **Advances in Space Research**, v. 35, p. 843-851, 2005.

LUMPKIN, R.; GARZOLI, S. L. Near-surface circulation in the tropical Atlantic Ocean. **Deep-Sea Research**, v. 52, p. 495-518, 2005.

LUTJEHARMS, J. R. E.; PENVEN, P.; ROY, C. Modelling the shear edge eddies of the southern Agulhas current. **Continental Shelf Research**, v. 23, p. 1099-1115, 2003.

MacCREADY, P.; GEYER, G. R. Estuarine salt flux through an isohaline surface. **Journal of Geophysical Research**, v. 106, p. 11629-11637, 2001.

MALANOTTE-RIZZOLI, P.; HEDSTROM, K.; ARANGO, H. G., HAIDVOGEL, D. B. Water mass pathways between the subtropical and tropical ocean in a climatological simulation of the North Atlantic. **Dynamics of the Atmosphere and Oceans**, v. 32, p. 331-371, 2000.

MARCHESIELLO, P.; McWILLIAMS, J. C.; SHCHEPETKIN, A. Open boundary conditions for long-term integration of regional oceanic models. **Ocean Modelling**, v. 3, n. 1-20, 2001.

MIRANDA, L. B. Forma de correlação T-S de massa de água das regiões costeira e oceânica entre o Cabo de São Tomé (RJ) e a Ilha de São Sebastião (SP), Brasil. **Boletim Mensal do Instituto Oceanográfico**, São Paulo, v. 33, n. 2, p. 105-119, 1985.

MOLINARI R. L. Observations of near-surface currents and temperature in the central and western tropical Atlantic Ocean. **Journal of Geophysical Research**, v. 88, p. 4433-4l38. 1983.

PENVEN, P.; ROY, C.; COLIN De VALDIERE, A.; LARGIER, J. Simulation and quantification of a coastal jet retention process using a barotropic model. **Oceanologica Acta**, v. 23, p. 615-634, 2000.

PENVEN, P.; ROY, C.; LUTJEHARMS, J. R. E.; COLIN De VALDIERE, A.; JOHNSON, A., SHILLINGTON, F.; FREON, P.; BRUNDRIT, G. A regional hydrodynamic model of the southern Benguela. **South African Journal of Science**, v. 97, p. 472-476, 2001a.

PENVEN, P.; LUTJEHARMS, J. R. E.; MARCHESIELLO, P., ROY, C.; WEEKS, S. J. Generation of cyclonic eddies by the Agulhas current in the lee of the Agulhas bank. **Geophysical Research Letters**, v. 27, p. 1055-1058, 2001b.

PETERSON, R.G.; L. STRAMMA. Upper-level circulation in the South Atlantic Ocean. **Progress in Oceanography**, v. 26, p. 1-73, 1991.

PREISENDORFER, R. W. **Principal component analysis in meteorology and oceanography**. Elsevier. Amsterdam. 1988.

RHEIN, M.; STRAMMA, L.; SEND, U. The Atlantic Deep Western Boundary Current. Water masses and transports near the equator. **Journal of Geophysical Research**, v. 100, p, 2441-2451, 1995.

RHEIN, M., STRAMMA, L. Seasonal variability in the Deep Western Boundary Current around the eastern tip of Brazil. Deep Sea Research Part I. **Oceanographic Research Papers**, v. 52, p. 1414-1428, 2005.

RODRIGUES, R. R.; ROTHSTEIN, L. M.; WIMBUSH, M. Seasonal variability of the South Equatorial Current bifurcation in the Atlantic Ocean: A numerical study. **Journal of Physical Oceanography**, v. 37, p. 16-30, 2007.

SCHMID, C.; SCHÄFER, H.; PODESTÁ, G.; ZENK, W. The Vitória Eddy and its relation to the Brazil Current. **Journal of Physical Oceanography**, v. 25, p. 2532-2546, 1995.

SCHMITZ Jr. W. J. On the interbasin-scale thermohaline circulation. **Reviews in Geophysics**, v. 33, p. 151-173, 1995.

SCHOTT, F.; BONING, C. W. The WOCE model in the western equatorial Atlantic: upper-layer circulation. **Journal of Geophysical Research**, v. 96, p. 6993-7004, 1991.

SCHOTT F.; J. FISCHER, J.; REPPIN, U. Send On mean and seasonal currents and transports at the western boundary of the equatorial Atlantic. **Journal of Geophysical Research**, v. 98, p. 14353-14368, 1993.

SCHOTT, F. A.; FISCHER, J.; STRAMMA, L. Transports and pathways of the upper-layer circulation in the western tropical Atlantic. *Journal of Physical Oceanography***,** v. 28, p. 1904-1928, 1998.

SCHOTT, F. A.; BRANDT, P.; HAMANN, M.; FISHER, J.; STRAMMA, L. On the boundary flow off Brazil at 5-10° S and its connection to the interior tropical Atlantic. **Geophysical Research Letters**, v. 29, n. 17, p. 21.1 – 21.4, 1840,, 2002. DOI:10.1029/2002GL014786.

SCHOTT, F. A.; DENGLER, M.; ZANTOPP, R.; STRAMMA, L.; FISCHER, J.; BRANDT, P The Shallow and Deep Western Boundary Circulation of the South Atlantic at 5°–11°S. **American Meteorological Society**, p. 2031-2053, 2005.

SHCHEPETKIN, A. F.; McWILLIAMS, J. C. Quasi-monotone advection schemes based on explicit locally adaptive dissipation. **Monthly Weather Review**, v. 126, p. 1541–1580, 1998.

SHCHEPETKIN, A. F.; McWILLIAMS J. C. A method for computing horizontal pressure-gradient force in an ocean model with a non-aligned vertical coordinate. **Journal of Geophysical Research**, v. 108, 35.1-35.34, 2003.

SHCHEPETKIN, A. F. McWILLIAMS, J. C. The regional ocean modeling system (ROMS): A split-explicit, free surface, topography-following-coordinate oceanic model. **Ocean Modelling**, v. 9, p. 347-404, 2005.

SILVA, A. C. **An analysis of water properties in the western tropical Atlantic using observed data and numerical model results**. PhD thesis, Department of Oceanography of the Federal University of Pernambuco, 2006. 135p.

SILVEIRA, I. C. A.; MIRANDA, L. B.; BROWN, W. S. On the origins of the North Brazil Current. **Journal of Geophysical Research**, v. 99, p. 22501-22512, 1994.

SILVEIRA, I. C. A.; SCHMIDT, A. C. K.; CAMPOS, E. J. D.; GODOI, S. S.; IKEDA, Y. The Brasil Current off the Eastern Brasilian Coast. **Brazilian Journal of Oceanography**, v. 48, n. 2, p. 171-183, 2000.

SILVEIRA, I. C. A.; CALADO, L.; CASTRO, B. M.; CIRANO, M.; LIMA, J. A. M.; MASCARENHAS, A. D. S. On the baroclinic structure of the Brazil Current-Intermediate western boundary current system at 22º - 23º S. **Geophysical Research Letters 31**, L14308: 1-5, 2004.

SMITH, W. H. F.; SANDWELL, D. T. Global seafloor topography from satellite altimetry and ship depth soundings. **Science**, v. 277, p. 1957-1962, 1997.

STRAMMA, L./ IKEDA, Y.; PETERSON, R. G. Geostrophic transport in the Brazil Current region north of 20° S. **Deep-Sea Research***,* v. 37, p. 1875-1886, 1990.

STRAMMA, L. Geostrophic transport of the South Equatorial Current in the Atlantic. **Journal of Marine Research**, v. 49, p. 281-284, 1991.

STRAMMA, L.; FISCHER, J.; REPPIN, J. The North Brazil Undercurrent. **Deep-Sea Research I** v. 42, p. 773-795, 1995.

STRAMMA, L.; ENGLAND, M. On the water masses and mean circulation of the South Atlantic Ocean. **Journal of Geophysical Research**, v. 104, n. 20, p. 863–883, 1999.

STRAMMA, L.; SCHOTT, F. The mean flow field of the tropical Atlantic Ocean. **Deep-Sea Research**, v. 46B, p. 279–303, 1999.

STRAMMA, L.; FISCHER, J.; BRANDT, P.; SCHOTT, F. Circulation, variability and near-equatorial meridional flow in the central tropical Atlantic. In G. J. Goni, P. Malanotte-Rizzoli. **Interhemispheric water exchanges in the Atlantic Ocean**, Elsevier B. V.,

2003. p.1-22,

STRAMMA, L.; RHEIN, M.; BRANDT, P.; DENGLER, M.; BÖNING, C.; WALTER, M. Upper ocean circulation in the western tropical Atlantic in boreal fall 2000. **Deep-Sea Research**, v. 52, p. 221–240, 2005.

VAUTARD, R.; YIOU, P.; GHIL, M. Singular spectrum analysis: a toolkit for short, noisy chaotic signals. **Physical D**, v. 58, p. 95-126, 1992.

Von SCHUCKMANN, K. **Intraseasonal variability in the southwestern and central tropical Atlantic Ocean**. Dissertation. 2006.

WITTER, D. L.; GORDON, A. L. Interannual variability of South Atlantic circulation from 4 years of TOPEX/POSEIDON satellite altimeter observations: WOCE South Atlantic Results. **Journal of Geophysical Research**, v. 104, n. C9, p. 20927-20948, 1999.

WÜST, G. Schichtung und zirkulation des Atlantischen Ozeans. Die Stratosphäre des Atlantischen Ozeans. Wissenschaftliche Ergebnisse Deutschen Atlantischen Expedition auf dem Forschungs und Vermessungsschiff. "**Meteor**" 1925-1927, 6, 109-228, 1935.